PWR FUEL ASSEMBLY OPTIMIZATION USING ADAPTIVE SIMULATED ANNEALING COUPLED WITH TRANSLAT

A Thesis

by

TIMOTHY JAMES ROGERS

Submitted to the Office of Graduate Studies of
Texas A&M University
in partial fulfillment of the requirements for the degree of

MASTER OF SCIENCE

August 2008

Major Subject: Nuclear Engineering

PWR FUEL ASSEMBLY OPTIMIZATION USING ADAPTIVE SIMULATED ANNEALING COUPLED WITH TRANSLAT

A Thesis

by

TIMOTHY JAMES ROGERS

Submitted to the Office of Graduate Studies of
Texas A&M University
in partial fulfillment of the requirements for the degree of

MASTER OF SCIENCE

Approved by:

Chair of Committee,	Jean C. Ragusa
Committee Members,	William S. Charlton
	Alexander Parlos
Head of Department,	Raymond Juzaitis

August 2008

Major Subject: Nuclear Engineering

ABSTRACT

PWR Fuel Assembly Optimization Using Adaptive Simulated Annealing

Coupled with TransLAT. (August 2008)

Timothy James Rogers, B.S., Texas A&M University

Chair of Advisory Committee: Dr. Jean C. Ragusa

Optimization methods have been developed and refined throughout many scientific fields of study. This work utilizes one such developed technique of optimization called simulated annealing to produce optimal operation parameters for a 15x15 fuel assembly to be used in an operating nuclear power reactor. The two main cases of optimization are: one that finds the optimal ^{235}U enrichment layout of the fuel pins in the assembly and another that finds both the optimal ^{235}U enrichments where gadolinium burnable absorber pins are also inserted. Both of these optimizations can be performed by coupling Adaptive Simulated Annealing to TransLAT which successfully searches the optimization space for a fuel assembly layout that produces the minimized pin power peaking factor. Within given time constraints this package produces optimal layouts within a given set of assumptions and constraints. Each layout is forced to maintain the fuel assembly average ^{235}U enrichment as a constraint. Reductions in peaking factors that are produced through this method are on the order of 2% to 3% when compared to the baseline results. As with any simulated annealing approach, families of optimal layouts are produced that can be used at the engineer's discretion.

ACKNOWLEDGEMENTS

I would like to thank my committee chair, Dr. Jean Ragusa, for fostering a very productive learning environment as well as being a personal friend throughout my entire time of knowing him. I would also like to thank my committee members, Dr. Charlton, Dr. Parlos, and Dr. Adams, for their contributions and guidance during the course of this research.

Thanks also go to my friends and colleagues and the department faculty and staff for making my time at Texas A&M University a great experience. I also want to extend my gratitude to Duke Energy and, in particular, Dr. Stephen Schultz and Mr. Robert St. Clair who have helped tremendously in not only funding the research project but also guiding me along the way in developing the method as well as presenting the work in a scholarly and professional manner.

Finally, it is with deep gratitude that I thank my mother and father for their undying support, encouragement, and love, without whom none of this work would be possible.

TABLE OF CONTENTS

Page

Page

LIST OF FIGURES

Page

Page

LIST OF TABLES

Page

1. INTRODUCTION: LITERATURE REVIEW

1.1 INTRODUCTION TO LIGHT WATER REACTOR FA OPTIMIZATION

Many studies for devising optimal operational conditions for Fuel Assemblies (FAs) have been previously performed, both at universities and in the nuclear industry. Both deterministic and stochastic methods are in use for the FA optimization problem, each with their own advantages and disadvantages. Deterministic optimizations often rely heavily on an initial guess, and their solutions can be highly sensitive to system perturbations, with stability concerns being omnipresent (Haibach and Feltus 1997; and Zavaljevski 1990). Despite these shortcomings, they generally require short simulation times and may provide a reasonable initial guess close to the optimum. This can provide an initial search domain to stochastic methods or serve as a guide to engineers in making design decisions. On the other hand, stochastic methods can better ensure finding a global optimum with high fidelity. The downfall of stochastic methods is the time it takes for such methods to complete. Run time can be reduced in stochastic methods but statistical measurements must be inserted to assess the validity of the results and global optima are not always ensured. The work reported in this Thesis is focused on finding the close-to optimal stochastic solutions for several specific cases of FA optimization, including a FA with radially graded enrichment in ^{235}U and a FA containing gadolinium as a burnable absorber. The first case is a FA where the ^{235}U enrichment of each of the fuel pins in the FA is varied to produce the lowest peaking factor attainable within a

---

This thesis follows the style of Annals of Nuclear Energy.

reasonable amount of time. This case allows a split feed enrichment FA with three possible enrichments. The second case allows an additional fuel pin type that contains gadolinium as a burnable absorber. Only a specified number of fuel pins that contain gadolinium are allowed with specific properties.

In order to perform these studies, several reviews of current knowledge will be summarized to establish the current working knowledge base. These reviews include surveys of available burnable absorbers, FA optimization methods currently in use, and heuristic approaches available. Surveys performed will serve to develop the knowledge necessary to properly develop the method proposed here.

1.2 CURRENT FUEL ASSEMBLY ENRICHMENT SCHEMES

Current available literature related to reactor optimization methods is extensive in many technical areas. Studies performed previously cover methods of finding optimal operational parameters for both Boiling Water Reactors (BWRs) and Pressurized Water Reactors (PWRs), the two main types of power reactors in operation in the United States and throughout the world. For both reactor types, BWR or PWR, a typical classification of the optimization paradigms used can be made as follows: in-core optimization techniques and out-of-core optimization techniques. Examples of out-of-core nuclear fuel management decisions include fuel assembly composition and the number of fresh fuel assemblies, utilization of burned assemblies, and prediction of performance over several campaigns (multi-cycle analysis). The other branch of the design space consists of the in-core nuclear fuel management strategies, such as the placement of the fresh and burnt fuel assemblies in the core to maintain safety and criticality constraints. With

mostly two reactor types in operation in the United States and both in-core and out-of-core optimization methods, this leads to four main areas of study for FA optimization. BWR reactor optimization methods are extensive and previous work done includes both in-core and out-of-core methods. Out-of-core methods in place (Martin-del-Campo et al. 2007) produce optimal enrichment grading of the fuel assembly by modifying enrichment of ^{235}U of each of the fuel pins to attain optimal performance characteristics desired. In-core methods (Castillo et al. 2004) shuffle available FAs to produce optimal reload designs. Additionally, burnable absorbers are used in BWR optimizations to increase burnup cycles by controlling reactivity excesses present at beginning of cycle (BOC). These methods include both stochastic and deterministic methods and are in use currently at several major nuclear industry companies such as General Electric and Areva (Sanders and Wagner 2002; Wagner and Parks 2002). Methods employed on the stochastic search branch include genetic algorithms, fuzzy logic, and tabu search techniques. Most deterministic methods in use provide the designer with only a best guess of the optimal solution, ultimately leaving the designer with the task of selecting how the solution effects changes to implement into the design. With such extensive work in place on BWR designs, natural motivations are present to produce similar methods for PWRs. Through the literature search performed on available methods for PWR designs, there seems to be significantly less work available in the out-of-core optimization for PWRs. Most of the PWR studies are related to in-core methods and methods developed are currently being utilized at nuclear firms such as Duke Energy, Areva, and Westinghouse. In-core methods for PWRs are similar to those in BWR

designs, but most notably include mainly simulated annealing (SA) and genetic algorithm (GA) techniques. Software packages available in this area as listed in Turinsky and Parks (1999) include but are not limited to FORMOSA, PANTHER, SIMAN, ROSA, and ALPS. Objectives of such codes include minimization of feed enrichments and burnable absorber material needed while maintaining peaking factor and temperature coefficient constraints.

As noted earlier, studies of out-of-core PWR optimization have not yet generated the same interests as in-core PWR methods or BWR methods. Several PWR works found in the literature were based on trial and error approaches, e.g., the master's thesis work of Caprioli (2004) at the Chalmers University of Technology, but these optimization techniques are not robust, fully developed methods that can be utilized currently by design engineers. Nevertheless, Caprioli's (2004) studies have shown the potential benefits that can be gained by properly varying the radial enrichment of ^{235}U throughout the FA to control performance characteristics and improve fuel utilization. It is also fairly common knowledge that some designs used by the nuclear utilities have enrichment modifications within the fuel assembly at specific locations to mitigate known issues: for instance, corner pins often have reduced enrichment content. This further strengthens the idea that out-of-core PWR optimization should benefit from more exploration than what has been performed to date. The work presented here aims at performing such an analysis for out-of-core PWR optimization in order to better understand the gains that can be obtained.

1.3 BURNABLE ABSORBER OPTIONS

Burnable absorbers are commonly used in PWRs and BWRs to control core reactivity and to enhance fuel performance. They capture neutrons during their burnout cycle and thus reduce the reactivity of a FA for a certain length of time that is proportional to the rate at which the primary absorbing isotopes are transmuted to other isotopes through absorption and decay. This rate is obviously dependent on the cross sections of each of the highly absorbing isotopes. Being able to absorb more neutrons at the beginning of cycle allows loading more ^{235}U in a fuel assembly so that the FA's cycle time can be extended. Another consideration in looking at burnable isotopes is decay chains. The decay chain of certain isotopes may contain very long lived products that would be undesirable. A survey of previously implemented burnable absorbers was performed and is discussed below.

Several burnable absorber implementations have been developed by PWR nuclear fuel vendors such as Westinghouse, B&W, Areva, and Combustion Engineering (CE) (Sanders and Wagner 2002). The two categories that burnable absorbers fall into are burnable poison rods (BPRs) and integral burnable absorbers (IBAs) as described in (Wagner and Parks 2002). BPRs are rods containing neutron absorbing material that are inserted into guide tubes of PWRs. They are commonly used for reactivity control for enhancing fuel utilization. IBAs refer to burnable poisons that are not removable or are an integral part of the fuel assembly. These also control reactivity for fuel utilization. There are four types of IBAs in manufacturing: integral fuel burnable absorber (IFBA™) rods, gadolinium (Gd) IBAs, erbium IBAs, and boron based IBAs. The difference

between the IFBA™ and the IBA pins can be visualized as in Figure 1. Westinghouse's IFBA™ is a rod with a thin coating of zirconium boride on the outer surface of the fuel pin. This burnable coating on the fuel can be varied in thickness to meet specific goals, while the number of these pins in a given assembly is varied over a range of 8 to 156 rods out of 264 fuel rods (Sanders and Wagner 2002). That represents up to 60% of the

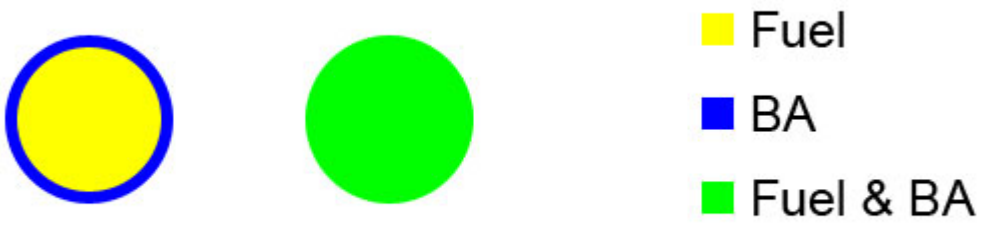

Figure 1 - IFBA™ vs IBA conceptualization with IFBA™ on the left and IBA on the right

rods of the assembly. Burnable absorber designs must satisfy a whole host of constraints and pass many tests before they can be declared useable, where such tests also include dry cask storage reactivity results. Studies performed at Oak Ridge National Lab (ORNL) for dry cask storage compared the k_{inf} values of assemblies with IBAs to the reference assembly k_{inf}, where a lower k_{inf} for the IBA assembly means that burnup credit criticality safety analyses may conservatively neglect the IBA presence. Usage of an IFBA™ assembly might produce reactivity higher than the reference

assembly in two dimensional results, but when three dimensional calculations were performed the axial burnup pulled the assembly reactivity below its reference (Wagner and Parks 2002). The other three types of burnable absorbers (BAs) all produce conservative results in the two dimensional cask studies. Manufactured previously by

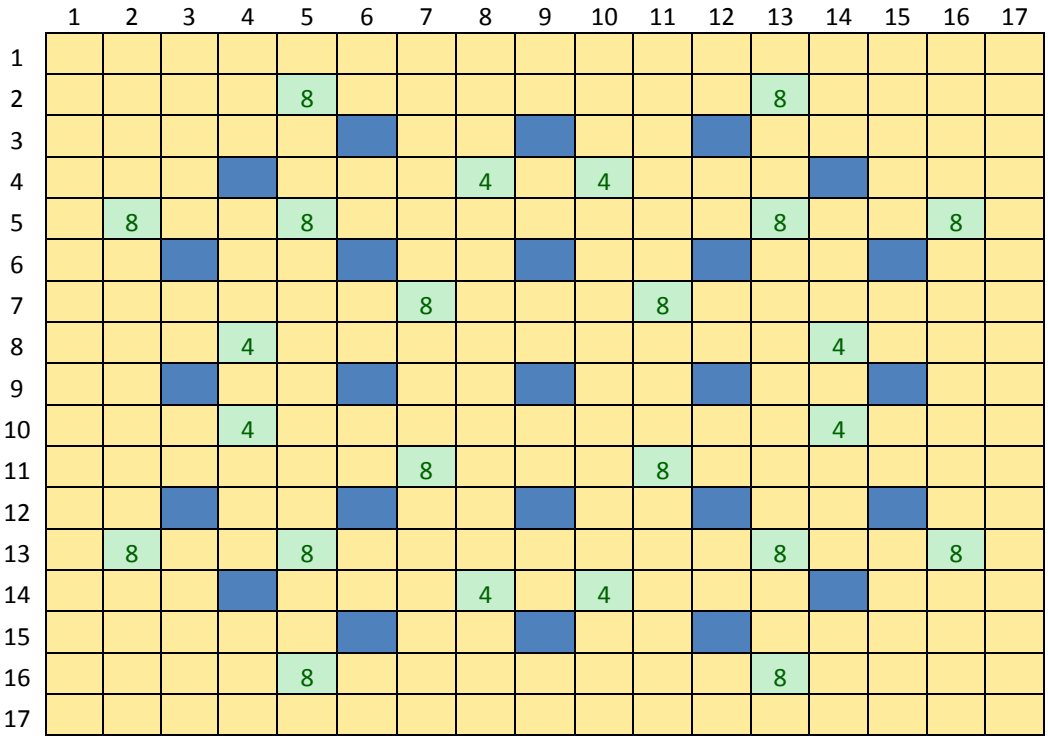

Figure 2 - Example BA layout for Gd-pins with 8 and 4 w/o Gd adapted from Sanders and Wagner (2002)

CE and Siemens and currently by Areva, Gd IBAs are pins that have a mixture of UO_2-Gd_2O_3 with the Gd_2O_3 present in varying w/o (weight percent) enrichments. Along with the enrichment of Gd_2O_3 in each pin, the number of pins in a FA can also be varied.

Some example layouts that have been produced for these types of BA implementations can be seen in Figure 2 and Figure 3. Often times the ^{235}U enrichment is reduced in the IBAs to satisfy heat conductivity issues presented by the addition of Gd in the fuel oxide as in (Sanders and Wagner 2002). Similar to the Gd bearing fuel pin is CE's erbium pin

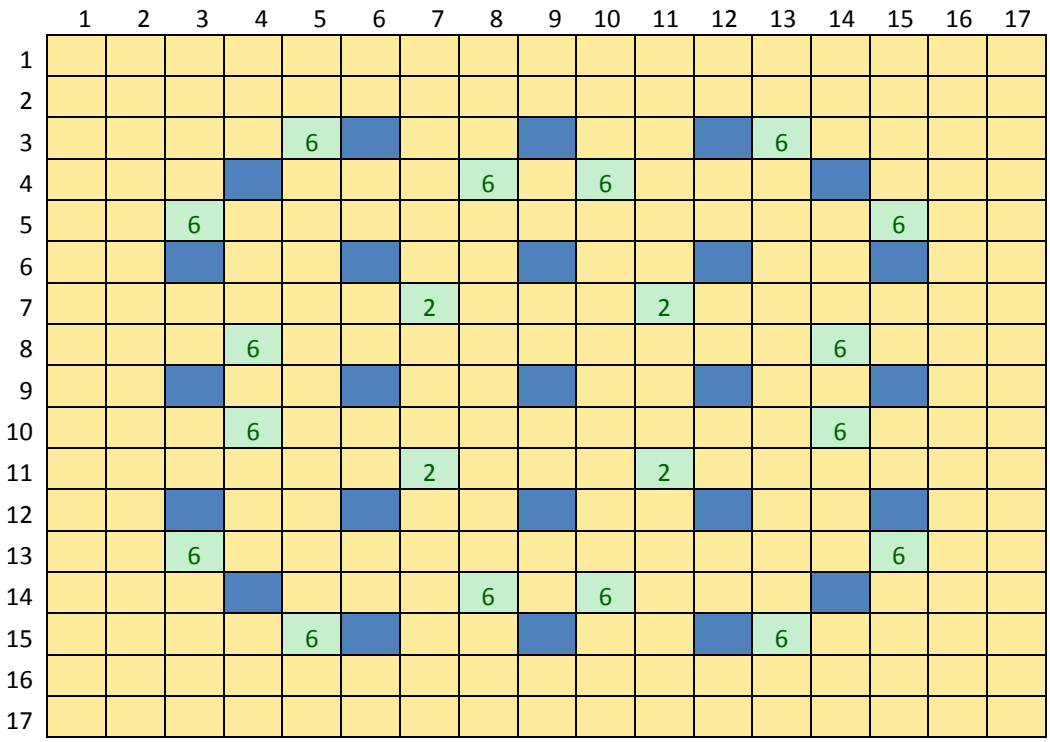

Figure 3 - Example BA layout for Gd-pins with 6 and 2 w/o Gd adapted from Sanders and Wagner (2002)

with variable enrichment and variable number of pins inserted in available designs. These two rare earth metals decrease the heat conductivity of the fuel matrix proportionally with the amount of the metal. Often times discussion goes into separating important isotopes of each of the metals as in (Grossbeck et al. 2003) such as ^{155}Gd,

^{157}Gd, and ^{167}Er that are both highly absorbing and do not have long decay chains. The strategy being implemented here is that removal of the excess isotopes in either erbium or Gd decreases the total volume taken up by the earth metal, leaving volumetric space for more fuel and also limiting the reduction in heat conductivity. Although this is a good strategy, the enrichment of the earth metals in their respective isotopes introduces an additional factor in the optimization and in the financial model. Introduction of these additional factors in subsequent studies could be examined; the present work limits the focus to IBA pins with naturally enriched Gd. Thus, these studies will be limited to naturally enriched earth metals to develop the optimization method. Also previously manufactured by CE, the fourth IBA rod is the solid rod containing alumina pellets with uniformly dispersed boron carbide particles (Al_2O_3-B_4C) clad in zircaloy. These rods, in contrast with the other IBAs, do not contain fuel. They do, however, fit into the IBA category since they are not removable from the FA. Variables for these pins include w/o of the B_4C and number of rods per assembly. These are pins that are not removable from the FA and thus are considered integral.

The other category of poisoning options is the BPR. Westinghouse makes two assemblies in this category, the Pyrex burnable absorber assemblies (BAAs) and wet annular burnable absorber (WABA). The BAAs contain a borosilicate glass Pyrex tube with a void in the center and clad in stainless steel. WABAs are similar but contain alumina boron carbide pins that are filled with water in their central void. Each implementation varies in number of rods from 4 to 24. Since this category of poisoning is limited to the water hole locations, it will not be used in this study.

In order to narrow the field for the type of burnable absorbers that can be used in this analysis, several available materials can be discussed. Materials reviews have been performed before on the most viable rare earth metals available. A comprehensive study was carried out at the University of Tennessee by Grossbeck et al. (2003) on material composition that aids in determining the most useful materials with given constraints. Material enrichment concerns encompass how the isotopics of the burnable absorber will affect the fuel matrix and the effects it has on the assembly itself when considering reactivity and peaking. Specific isotopics of burnable absorbers to be used can be chosen based on material limitations as well as financial goals. There are varied types of pins that have been developed. These include coating the fuel pin with burnable absorber, mixing the burnable absorber with the fuel itself, and inserting burnable absorber into the water hole locations. Each of these has their own advantages and disadvantages.

In order to analyze available materials, the list of available elements is limited to a short list of neutron absorbing materials. Generally mentioned as burnable absorber materials are Gd, samarium, erbium, europium and dysprosium. Each of these is a rare earth metal that has little abundance in natural environments, with europium being the rarest (Asou and Porta 1997). Based on single isotope burnable poison studies, each of these are viable candidates. However, not all of these are currently economically feasible due to manufacturing costs and handling difficulties. Samarium is not useable because of its reactivity and its low boiling point; europium is not used because of its less favorable nuclear properties. Nuclear properties to consider are primarily the

metal's decay scheme and absorption characteristics of daughter nuclides produced. Decay chains of several of these metals contain very highly absorbing daughters that loop back to other highly absorbing nuclides leaving a large reactivity residual. The ideal burnable absorber material controls excess reactivity over a specified time range and then disappears from the physics picture. That is to say it soaks up neutrons for a period of time, and then it and its daughters stop absorbing neutrons and allow the fuel to dominate neutron absorption. This leads to the lowest reactivity residual effect, which is desirable. Dysprosium has a very long decay chain with several isotopes that are hard to burn. Taking this into account leaves only Gd and erbium in the list of possibilities as supported in Asou and Porta (1997). For this study, Gd is the most suitable since peaking factor control is only needed for a short amount of time. The reasoning behind the time period that Gd is needed stems from the fact that the peaking factors in the FA only need to be reduced by the Gd for only several burnup steps and then need to go away. Gd burnup rate is optimal for cycle lengths on the order of one to two years where natural erbium burns at a linear rate for up to four years. This can be seen in Figure 4. It can be used in a low number of rods and at high contents. Gd also exhibits a unique behavior in that the number of poisoned rods controls the negative reactivity while the content controls the length of the burn-up kinetics almost independently as shown in (Sanders and Wagner 2002). Gd material specifics such as enrichment are the next choice to make. Several Gd enrichments have been used when implementing Gd oxide as a burnable absorber material. Enrichments vary from as low as 2%, which is

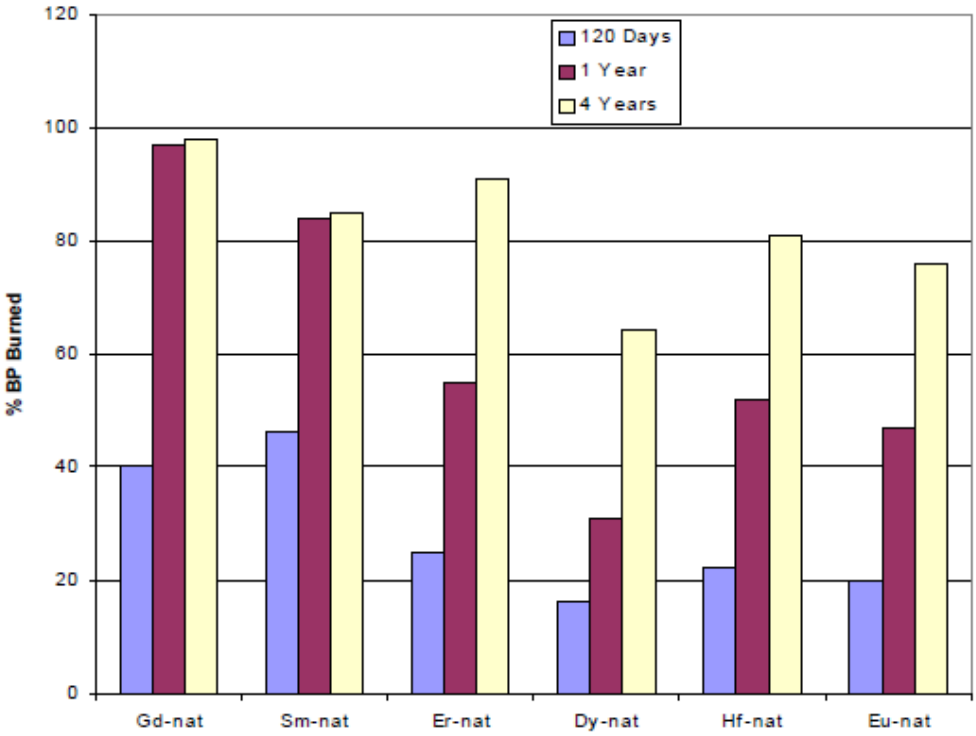

Figure 4 - Percentage of burnable poison burned at the end of each specified time period for the naturally occuring elements mixed in outer third of the fuel rod volume as given in Grossbeck (2003)

what is referred to as natural Gd, to 12%. The specific isotopes of Gd that are highly absorbing are ^{155}Gd and ^{157}Gd. Each of these isotopes has large capture cross sections for neutrons in the fast spectrum. Since there is such a wide range of successful enrichment choices, determining a nominal enrichment becomes either a blind choice of fanned cards, or a median value for a starting point, or another parameter to be optimized. The median value chosen is 6% Gd enrichment; subsequent studies could be carried out to fine tune this value using the framework developed in this thesis. This parameter can be studied for its own feasibility but the optimization is to find optimal

layouts with given assumptions, with this enrichment being one of the initial conditions. This choice is the IBA pin that will be placed in the FA with a composed layout. Although many studies have gone into optimal Gd pin placement, there were not any available with the same water hole layout as the specified design. The nominal IBA layout that will be used has twenty burnable poison pins and was selected as the nominal layout because it controls the peaking factor to a satisfactorily low initial condition that can be correlated with similar pin designs. It is possible to argue alternatives to these decisions but it is important to keep in mind that the optimization method being used here treats the simulated system as a black box and thus these assumptions can be updated as needed. The purpose of this work is to demonstrate a PWR fuel assembly optimization methodology, with applications to Gd-bearing and non Gd-bearing fuel assemblies as validation of the methodology. It is envisioned that subsequent studies may fine tune a number of parameters that are presently fixed. This optimization method may be similar in scope to existing applications, but it does differ in both the objectives and the implementations used.

1.4 FA OPTIMIZATION METHODS IN USE

Available optimization methods include stochastic methodologies along with deterministic solutions. Due to the highly complex and nonlinear nature of any given FA optimization, the methods for optimizing system parameters usually require both computationally expensive calculations and simplifying assumptions about system behavior. Stochastic methods currently in use for fuel management optimizations include genetic algorithms, tabu search, neural networks, and simulated annealing

(Yilmaz et al. 2005; Castillo et al. 2004). System parameters used in these types of optimizations include fuel enrichments, burnable poison locations and enrichments, and fuel positioning. The GA premise is that a gene can correspond to an input string of system variables that represent the variables to optimize. This method is based on Darwinian evolution theory and uses a "survival of the fittest" principle where fitness assessment is measured by a predefined objective function. The algorithm breeds new genes by using methods that resemble biological breeding. Other techniques in use behave similarly, utilizing the same operational parameters albeit in different ways with differing motivations. Tabu search is a local search method that marks the locations that it has visited to effectively remember the solution at that location. Once the method visits a certain point in the space then it does not visit that point again but remembers the solutions obtained. This method can help to reduce run time in global sampling methods. Neural networks (NN) utilize an interpretation of how the human brain stores information. They use networks of nodes to learn how a system transforms input to output vectors and try to mimic that behavior. SA has been coupled to lattice-physics codes in order to optimize common system parameters and has physical motivations as well. The search method in simulated annealing randomly generates each proposed solution and thus is computationally expensive. This method uses generating distribution functions, acceptance distribution functions, a temperature schedule, and both initial and final temperatures to perform its search of the problem domain until it finds a global optimum. If the simulated annealing process is granted an infinite amount of time to search the domain, it will find the global optimal results, but this is neither

feasible nor interesting. The algorithm of an SA code produces an input vector randomly using its generating distribution and then accepts or rejects the proposed input vector based on the acceptance criteria. Acceptance of an input vector is based on the system temperature and the heuristic rules. This process of generating acceptable input vectors is then repeated while the temperature of the system is lowered according to the cooling schedule. Generally exponential functions are used to establish proper cooling schedules. This allows for large variations in the initial phases of the optimization so that the algorithm can sample large spaces to find the optimal region. It is desirable to find this optimal region and then search within that region for the optimal solution. The search method can find global optimal values given a certain set of characteristics. The formal heuristic statistical proof of finding the global optimum is given in Adaptive Simulated Annealing (ASA) documentation (Ingber 2007) as such:

The parameter temperature schedules must suffice to insure that the product of individual generating distributions, *g* for each parameter indexed by *i*,

$$g = \prod_i g^i \tag{1}$$

taken at all annealing times, indexed by *k*, of not generating a global optimum, given infinite time, is such that

$$\prod_k \left(1 - g_k\right) = 0 \tag{2}$$

which is equivalent to

$$\sum_k g_k = \infty \tag{3}$$

For the ASA temperature schedule, with dimension *D*, this is satisfied as

$$\sum_{k}\prod^{D} 1/k^{-1/D} = \sum_{k} 1/k = \infty \quad (4)$$

Now, if the temperature schedule above with temperature T and initial temperature T_0, is redefined as

$$T_i\left(k_i\right) = T_{0i}\exp\left(-c_i k_i^{Q/D}\right) \quad (5)$$

$$c_i = m_i \exp(-n_i Q/D) \quad (6)$$

in terms of the "quenching factor" Q, and the two scaling factors m and n indexed over the parameters involved by i, then the above proof fails if Q >1 as

$$\sum_{k}\prod^{D} 1/k^{-Q/D} = \sum_{k} 1/k^{Q} < \infty \quad (7)$$

Depending on the system being optimized and the number of parameters, quenching can provide a faster way to find optimal solutions but does not guarantee that it is the global optimum. A key element in developing a feasible simulated annealing approach is in developing a cost schedule that provides the global optimum in a reasonable amount of time as well as adaptively choosing how the problem domain is searched so that the proper valleys are explored thoroughly but quickly.

Before any of these techniques are utilized, however, manual trial and error optimizations of the fuel parameters serve to develop the system knowledge necessary to assess the success or failure of more robust methods. Performing these types of manipulations is somewhat limited to the foresight and intuition of the designer to think of an optimal layout. This type of work has been performed by Caprioli (2004), where

she explores the effects of varying the enrichment of each of the fuel pins in the selected FA to obtain flatter internal peaking factor distributions to the fuel assemblies as well as to extend cycle lengths. Although inspiration was drawn from BWR fuel management solutions, the PWR axial moderator phase is uniform and thus does not affect the fuel heat removal quite like that experienced in the BWR design. For this reason, it is not necessary to vary the axial enrichment through the active fuel length. There are, however, axial blankets like those used in most typical PWR designs. It is important to note that Caprioli's work suggests that limitations be set on the enrichment change values. The pin power is driven to the pins with the highest differential enrichment in the FA, and thus the FA internal peaking factor is driven solely by the highest enrichment allowed. Limitations of her work exist in the "by hand" approach, thus limiting the number of cases developed. In general the study does provide some motivation to fully develop a robust optimization method that can confirm her findings with the intention to enhance the results.

GAs have been applied to both PWR and BWR designs to find optimal burnable poison placement and loading. One such BWR GA application (Martin-del-Campo et al. 2007) uses a code called HELIOS to search for a fuel lattice with the lowest average enrichment satisfying target reactivity, local peaking factor, and average gadolinium concentration. Notable components of this work are that it is done in two dimensions, half diagonal symmetry is used, and calculations of the peaking factor and reactivity results are performed at burnup step zero. They propose that good reactivity performance during lattice exposure can be assured in their FA if the average enrichment

change is limited (Martin-del-Campo et al. 2007). An objective function was developed that takes into account each of the gadolinium loading, the reactivity, and the peaking factor for the FA. Each of these components is weighted based on the assumed importance of each factor. In order to limit the search space, they do not allow gadolinium to be placed in locations along the edge of the FA and assume that the corner positions will contain the lowest enriched fuel pins in the optimal solution. They find that GA methods are suitable to apply to this type of optimization and that if the average enrichment reduction is limited then extensive burnup lattice calculations are not necessary to assure good reactivity performance. Another application of GA pertains to PWR designs as performed in (Yilmaz et al. 2005). In it they vary the number of gadolinium pins and associated gadolinium concentration with the total amount of gadolinium as the objective function. The main objective of the work is to find a burnable poisons loading pattern that minimizes total gadolinium in the core while maintaining peaking factors and soluble boron concentrations below established limits. This work, however, is performed at the core level and uses specific FAs from a list of available FAs to place in locations throughout the core to meet the problem objectives. They find that GA is suitably applied at this level of optimization and suggest several cost effective designs that could be implemented given that their assumptions are satisfied. These two works show the applicability of GAs as optimization techniques and establish several very important assumptions that can be made when performing FA optimizations. As for Tabu search techniques, an application of this search method was applied with heuristic rules of Control Cell Core and Low Leakage as in Castillo et al.

(2004). Their objective was to maximize the cycle length while satisfying the operational thermal limits. This work was done at the core level and thus places available FAs in an octant of a BWR core. Assumptions such as not allowing fresh FA placement along the periphery as well as not allowing fresh fuel in control rod locations are implemented. The method is able to find a loading pattern of the FAs to satisfy their constraints allowing for 34 more days of full power operation. They suggest that future work includes implementing the search of optimized control rod patterns. This work illustrates a successful application of tabu search methods to core level optimization. Lastly is the work done by Maldonado et al. (1998) to develop dual-objective simulated annealing to apply to lattice loading optimization as well as the penalty-based constraints implemented in Maldonado (1998). This work looks at FORMOSA-L's ability to optimize spatial distributions of enrichment and burnable absorbers within a FA. FORMOSA-L is a SA optimization code that can enforce relative power peaking constraints as well as reactivity constraints to search for a global optimal solution as discussed in Maldonado et al. (1998). This work suggests that implementation of dual-objectives or penalty-based constraints can improve upon results of single-objective constraints. They combine both power peaking minimization and FA enrichment into an objective function that is stabilized by natural logarithm normalizations so that the log of the product of the two objectives is minimized. Important notes on this work are that a three-enrichment split allowance is made and the assembly average k-infinity was constrained to ± 200 pcm relative to the reference assembly. These assumptions perform well in their work and contribute to the building of assumptions necessary for

the method being applied here. These methods have been applied in their various partitions of the optimization process of designing power reactor cores. Assumptions made and results found indicate their viability and are taken into account when developing the method of this work.

2. BASELINE FUEL ASSEMBLIES

2.1 OPTIMIZATION AND THE NEED FOR BASELINE FA CASES

Analysis of optimization results is the key element in being able to interpret the results for real world implementations. To properly analyze optimization results, a reference baseline fuel assembly must be established from which all simulations can be compared. This optimization process aims to produce a FA that has more desirable performance characteristics than those of FAs that are being used currently at the Oconee Nuclear Station (ONS). As specified in several publically available documents, the FA used at ONS is a 15x15 FA which is used to develop the reference FA design that has no integral burnable poison and a spatially constant enrichment. Since this is what is being used, a direct definition of the baseline FA can be derived from this specification. Performance of this baseline FA will serve as the initial performance characteristic from which the optimization should improve. Alongside radial enrichment zoning optimization is the optimization that introduces Gd-pins to reduce reactivity over the initial burnup cycle. Since there is not a specification of a FA in use that utilizes Gd-pins, one is developed based on literature and engineering intuition. These baseline FA designs are provided in the following sections.

2.2 DEFINITION OF A STANDARD/BASELINE FA

The baseline FAs will be considered here: one baseline FA without Gd-bearing pins and another baseline FA with Gd-bearing pins. These baseline or nominal FAs will be used as a performance metric for the various optimized FA. The baseline FAs also

serve in defining some of the constraints in the optimization process (e.g., preservation of the average enrichment, same number of Gd pins, etc). The baseline FA used in all of the modeling is built from specifications from the UFSAR document (ONS UFSAR 2005) openly available for the Oconee Nuclear power plant operated by Duke Energy. The FA design is referred to as the Mk-B10 FA. Descriptions and assumptions are made through interpretations of the UFSAR document which may differ slightly from the actual FA (e.g., operating temperatures, fuel pin specifications, and material properties). Where room for interpretation was left to the designer, industry best practices were applied as rigorously as possible.

2.3 DESCRIPTION OF THE UOX FUEL ASSEMBLY (UOX, NON GD-BEARING FA)

Development of the baseline uranium oxide (UOX) FA consists mostly of verifying geometries, operating parameters, and assumptions made. It is important to note that results may vary based on a number of factors including assumptions made, neutronics code used, and optimization method followed. This FA is given an initial flat enrichment layout of 4 w/o ^{235}U. This enrichment will correspond to the average that is maintained throughout most optimizations unless otherwise noted.

Materials specifications are the major component to simulations. There is a short list of materials necessary to consider in the simulations but their specifications are key in obtaining correct results. Materials include cladding, fuel, and moderator. The cladding used is Zircaloy-4 as per the UFSAR. There is not a standard Zircaloy-4 material in the TransLAT library so the material used is composed of the major components present in Zircaloy-4. One important assumption to note here is that the

Zircaloy-4 material is being smeared over the fuel cladding gap present in the fuel pins to simplify calculations. The way this is done is by diluting the density over the combined areas of the clad and the fuel cladding gap with an area based weighting factor. Cladding density is specified to be 6.55 g/cc before smearing and then becomes 5.84 g/cc after the factor is applied. Primary elements present in the cladding are chromium, iron, and zirconium. This specification gives the properties of the cladding

Table 1 - Physical properties of fuel assembly

ρ_{UO2} (theoretical)	10.96	g/cm^3
ρ_{UO2} (calculated)	10.28	g/cm^3
reactor power	2568	MWt
core loading	93	MTU
# FA	177	
power per FA	14.5	MWt/FA
cells in FA	225	
# of water holes	16	
# IT	1	
# of fuel elements (FE)	208	
height of FE	140.6	
volume of FE	247.7	cm^3
volume of FA	51528	cm^3
mass UO_2 in FE	2547	g/FE
mass UO_2 in FA	529732	g/FA
mass UO_2 in FA	0.53	tonne/FA
power density	27.4	MW/tonne - HM
Zirconium 4 ρ	6.55	g/cm^3
Zirc-4 calculated ρ	5.84	g/cm^3

used in the fuel pins as well as the water hole and instrumentation tube (IT) locations. Material and some other necessary properties of the FA are given in Table 1.

Fuel materials are very standard input and generally need only a few parameters. The theoretical density of the UOX fuel is 10.96 g/cc. Fuel pins are not, however, manufactured to this density nor do they operate at this density due to in-reactor indensification. The density input for TransLAT is reduced to 10.28 g/cc based on calculations of these effects. The change in density is input as a percentage of theoretical density of 93.8%. Then the enrichment for the fuel is given as a nominal 4.00 w/o ^{235}U. Various other enrichments will be used over the scope of the optimization. The accepted ranges here are as low as 3.50 w/o ^{235}U up to 5.00 w/o ^{235}U. We wish to keep the reactivity of the FA above a certain threshold, so anything below 3.50 w/o will be atypical.

Moderator specifications are the last topic to discuss. Moderator properties are mostly based around the void fractions of the water present and the boron content. The material H_3BO_3 will be used as the boron material. Boron concentration varies as a function of fuel burnup during the cycle, but, for depletion purposes, an average value is typically used. Note that for core neutronics studies, the cross section libraries generated by the lattice code usually consist of the data obtained during the nominal depletion, but also contain the data obtained by varying fuel temperature, moderator temperature, and boron concentration for each burnup value. Such perturbations are the “branch cases” of the nominal depletion steps. We are not concerned with generating such cross section libraries and thus will only run the lattice code for depletion purposes. The average boron concentration is set to be 700 ppm of H_3BO_3 over all burnup steps. The FA described in the UFSAR document is a Mk-B10 FA that is a lattice of fuel pins

measuring 15x15 pins wide and deep. An assumption of this modeling is that 1/8th symmetry will be maintained and is sufficient to capture the behavior of the FA in its infinite lattice domain as can be seen in Figure 5. The FA consists of the lattice with an

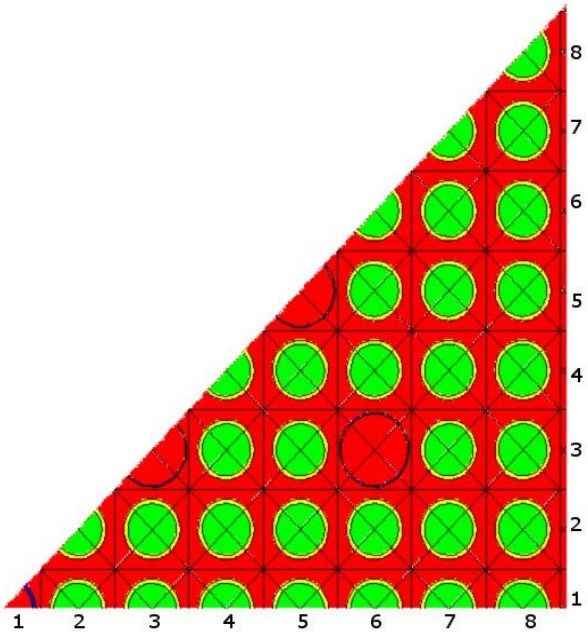

Figure 5 - Visual representation of 1/8th of the Fuel Assembly where red corresponds to water, green to fuel, and yellow to cladding

IT in the center and then sixteen water holes in a B&W FA design. This means there are 208 fuel pin locations. Each of the cells used in the lattice have dimensions as specified in Table 2. There is also a water gap present with the reactor at zero power. This gap dependent on the relative thermal expansion of the FA grid material to that of the core support structure. Modeling is done before this expansion occurs, i.e., at room

temperature. This assumption stems from standard practices as available to the designers and from literature.

As per the literature review of optimization methods in use (Martin-del-Campo et al. 2007), burnup (depletion) calculations are not needed during the optimization process and thus simulations are performed only at burnup step zero. Depletion calculations are an important part of analyzing results and thus are performed as a cursory step to display the solution behavior. The burnup steps will extend to 70 GWd/MT-HM under a

Table 2 - Physical dimensions of fuel assembly components as given in the ONS UFSAR (2005)

	in	cm
Fuel Element Pitch	0.568	1.4427
Fuel Pellet Diameter	0.37	0.9398
Inner FE Clad Diameter	0.377	0.9576
Outer FE Clad Diameter	0.43	1.0922
Inner IT Clad Diameter	0.441	1.1201
Outer IT Clad Diameter	0.493	1.2522
Inner Water Hole Diameter	0.514	1.3056
Outer Water Hole Diameter	0.53	1.3462
Inter - Assembly Gap	0.05	0.1270

predictor/corrector method. Since higher accuracy is needed initially in the burnup cycle, a finer grid is used early on with the mesh becoming coarser as time goes on. The mesh is as small as 0.25 GWd/MT-HM.

2.4 DESCRIPTION OF THE UOX-GD FA (UOX, WITH GD-BEARING PINS)

The other baseline FA to develop contains Gd-bearing fuel pins. This baseline is a necessary component of the optimization that utilizes the Gd-pins to serve as a result from which outputs can be compared. As per the literature review (Sanders and Wagner 2002), the Gd-bearing pins that will be used mix the Gd uniformly with the fuel at a specified weight percent. These rods are specified with the same theoretical density as normal fuel rods, lowered ^{235}U enrichment content, and a specified weight percent of gadolinium. Gadolinium enrichment can be modified by increasing the w/o of the two highly absorbing isotopes of gadolinium, ^{155}Gd and ^{157}Gd. Natural gadolinium enrichment contains 2 w/o 155/157. This is not to be confused with the Gd enrichment

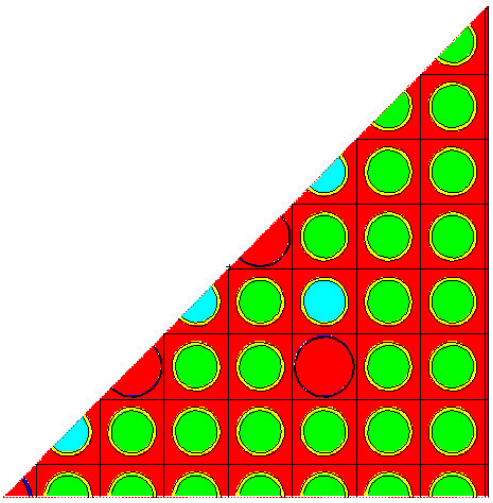

Figure 6 - Nominal IBA pin layout for baseline FA analysis with Gd-pins in blue and fuel in green

in the fuel pin which can vary up to 12 w/o Gd. Many studies have been done on how to best utilize gadolinium in fuel rods by dispersing the gadolinium into the fuel matrix evenly, and what has been found is that the gadolinium reduces the heat conductivity of the fuel and thus the enrichment of ^{235}U must be reduced to maintain safety limits. This reduction will be nominally set to 0.25% ^{235}U for all cases, unless specified. In developing the baseline model, Gd-pins that will be used will contain 6 w/o Gd and contain uranium fuel enriched to 3.75 w/o ^{235}U to minimize heat conductivity issues. These pins are placed in the FA as seen in Figure 6. This layout of the locations of the Gd-pins was developed from literature reviews of similar FAs in use along with design knowledge of the FA developed through previous studies.

2.5 VERIFICATION OF EXPECTED OUTPUTS

Calculations performed in the FA optimization must be entirely independent of the neutronics codes used. It is, however, useful to verify that the codes being used have expected results by performing code-to-code benchmarking. The described FA was built in TransLAT as well as in CASMO-4. CASMO-4 input decks have been verified before by Duke Energy and thus serve as a good benchmark to establish the validity of the TransLAT results obtained. CASMO-4 is an industry standard code optimized to produce results that are viable in the nuclear industry and thus has some simplifications and assumptions to guide the engineer towards conservative results that ensure the safe operation of reactors. The main output values that are compared are the peaking factor characteristics and the reactivity of the fuel pins both as a function of burnup. In order to get comparable results, all dimension calculations were checked along with

calculations of system parameters to ensure consistency. Although seemingly trivial, this task does require unit conversions and interpretations of each code's standard inputs so that the modeling is as comparable as possible. What was found in this analysis was that although there was some discrepancy between the results, they can be justified when taking into account the differing methodologies employed by each of the codes as well as slightly differing nuclear data files. The differences in results from each of the codes stems also from the purpose of each code.

Of primary interest to this study is the peaking factor result accuracy. Resulting peaking factors from TransLAT output seem to compare well with CASMO-4 results when doing non-Gd simulations. It has become apparent, however, that either the inputs of the two codes are not consistent enough at this time or the normalization schemes when introducing Gd-pins are not consistent linear transformations of each other. Further benchmarking could be useful in transitioning between the two lattice physics engines. The method produced here, however, is a black box method that is written independent of the lattice physics code, and, therefore, it is stressed that these results pertain only to TransLAT and that replacing the lattice physics engine may result in different solutions. Despite these drawbacks, when TransLAT peaking factor output is normalized to a similar constant to that of CASMO-4, the results are very close to each other. This can be seen in Figure 7. It is important to note that the general functional shape of the peaking factor versus time remains the same for both applications and thus only a linear shift in the results is needed to translate the results from one code to another for these baseline calculations. This shows that the codes are consistent in the reference

calculations that are being performed but that they are merely displayed differently. TransLAT peaking factor results can thus be considered consistent with CASMO-4 results and will be used in optimization analyses.

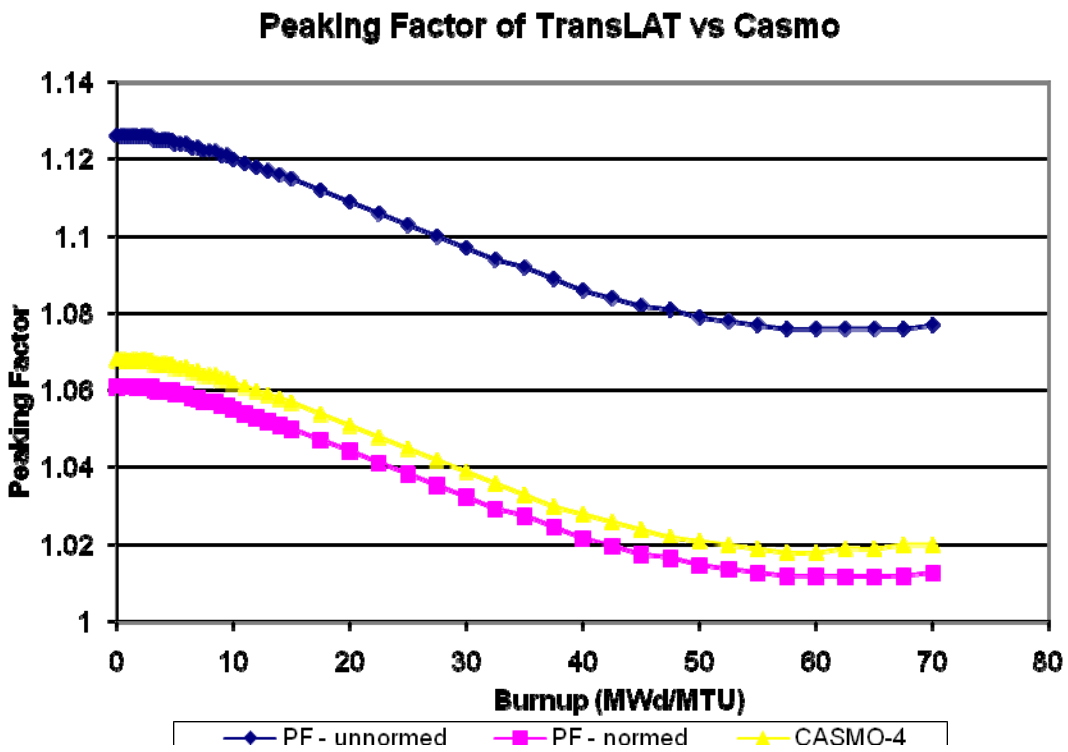

Figure 7 - Maximal peaking factor comparison of TransLAT normed and unnormed peaking factors to CASMO-4 peaking factors as a function of burnup

Reactivity is another important feature to help benchmark TransLAT to CASMO-4. When comparing reactivity of the two codes, it is useful to monitor the pcm difference from one code to the other. When this analysis was completed it was shown

that TransLAT stayed within ± 600 pcm of the results of CASMO-4. This could possibly be explained as the difference between setting the boron concentration as a constant versus having a functional change over time. This reactivity comparison is shown in Figure 8.

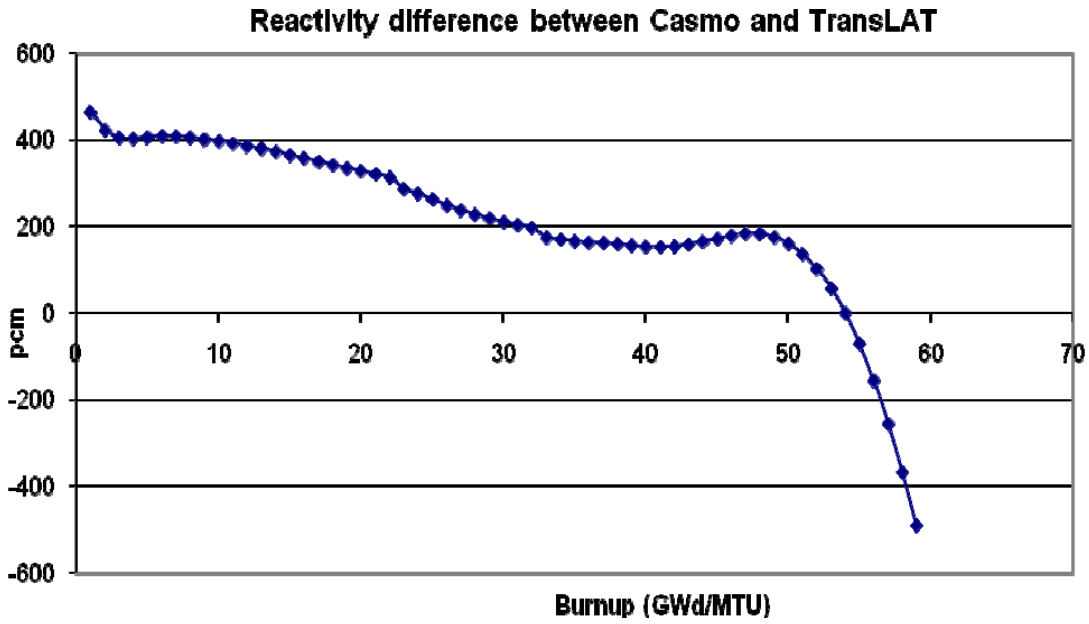

Figure 8 - Reactivity comparison of CASMO-4 and TransLAT using similar input decks

3. HEURISTIC OPTIMIZATION

3.1 INTRODUCTION TO HEURISTICS

A common definition for the term heuristic (serving as an aid to learning, discovery, or problem-solving by experimental and especially trial-and-error methods) effectively summarizes the term's application and implies the notion of repetition and learning by trial and error. A heuristic method will thus involve using repeated sequences to figure out a solution, where the number of attempts will be directly related to the ability of the engine to make better guesses based on previous knowledge. Here, this optimization process, or method, will attempt to accurately capture the behavior of the fuel assembly and explore the parameter space according to physical attributes and assumptions being applied. In order to do that, some initial rudimentary heuristic knowledge must be developed in order to properly implement the FA optimization process. Heuristic knowledge can be developed by trial and error variations within the variable space to see how the system responds to the variations. Knowledge developed from these variations can then be implemented into more robust optimization methodologies that have algorithms for performing the variable manipulations. The following sections describe both manual manipulations of the variable space that have been performed as well as robust methodologies available.

3.2 SIMPLE HEURISTICS

In order to get a sense of the manipulations an optimization technique might need to make, as well as to develop constraints to present to the optimization technique, it is

important to perform several heuristic optimizations or “by hand” optimizations. Numerous approaches can be taken when modifying a lattice’s enrichment layout scheme and numerous end results can be attained. The engineer may need a FA that minimizes the pin power peaking factor (PPPF) while constraining the overall reactivity of the FA during some specific lifetime, or may only need to reduce the PPPF to a certain value and then maximize the reactivity at the end of life (EOL) of the FA in order to prolong its overall cycle lifetime in the core. Several example schemes that can be implemented are, for example, constraining the “by hand” optimization to maintain an average enrichment over the FA or possibly varying the average enrichment while maintaining some other constraint such as reactivity and PPPF. Throughout the examples explored the simplest constraint to implement and most primary to study is to maintain a constant average enrichment while minimizing the maximal PPPF of the FA in order to study the reactivity effects at EOL of the FA. Several schemes were developed for the “by hand” optimization.

3.3 ONE TO ONE ENRICHMENT MODIFICATIONS

The first scheme developed is the most simplistic case and is called one to one enrichment modification. This is the case where the fuel pin with the highest peaking factor has its enrichment reduced by a given delta (e_δ), and then the pin with the lowest peaking factor has its enrichment increased by the same delta to maintain constant average FA enrichment. Peaking factors for this decision come from the map that is produced from the nominal flat enrichment case where all pins are 4.00 w/o ^{235}U. With the first pin pair chosen, a simulation is performed with the highest and lowest powered

pins' enrichments modified to obtain a new power peaking factor map (PPFM). This new PPFM is then used to make the next pin pair selection to reduce and increase enrichment as done in the previous step. The PPPF that is used to make modification decisions is the maximum PPPF over all of the burnup steps performed. It was determined that if the average FA enrichment remained constant in these simulations then the maximum PPPF at burnup zero can be treated as the maximal PPPF over the burnup cycle, and thus all decisions in this scheme can be made on the PPFM obtained at zero burnup. The decision to only utilize zero burnup PPFMs was made because of an assumption that was drawn in early tests of FA reactivity with respect to time as changes such as these were made. It was noticed that although the initial reactivity was variable, the final reactivity close to 60 GWd/MTU converged for all cases. With this assumption simulation time is drastically reduced. Two branch cases stemmed from this scheme. The differing paths depend on when the enrichment change decisions are made. Either the decisions can all be made *a priori* or they can be made after each step is chosen so that the next step can take into account the previous results. Both branches had the same resulting enrichment changes through almost all of the steps taken. The branches did begin to differ in resulting changes after 4-5 steps depending on the delta in enrichment change taken. This scheme proved to give insight into the optimization problem at hand, but several problems arose.

The simulation that is being performed assumes octant symmetry of the FA. This means that if an enrichment of a pin along the diagonal or the interior edge of the octant of the FA is changed, then that change is replicated only four times in the whole

FA. This contrasts with interior pin enrichment changes, which are replicated eight times. Thus a change in merely the max PPPF location may not equally correspond to a change in the min PPPF location when using constant average enrichment as a constraint.

3.4 MULTIPLE ENRICHMENT MODIFICATIONS

In order to further develop the heuristic knowledge for the optimization method, another plan was devised in which pin modifications are made so that the limitation of the one to one method can be removed. This allows for multiple pin enrichments to be modified per step taken. In the case that the corresponding max and min PPPFs do not coincide as interior or exterior pins, an additional pin pair must be modified to conserve the average enrichment of the FA. The development of this method helps reduce the limitations imposed by a symmetric design. Knowledge of how these pins need to be

	1	2	3	4	5	6	7	8
8								4
7							4.25	4.25
6						4	4.25	4.25
5						4	4	4.25
4				3.75	3.75	3.75	4	4
3				3.75	3.75		4	4
2		4	3.75	4	4	4	4.25	4
1		4	4	4	4	4	4	4

Figure 9 - Sample modifications made in heuristic approach

modified to approach an optimal assembly design helps develop optimization constraints necessary to determine the effectiveness of designs. The multiple enrichment modification plan shows the designer that it is not necessary to approach the optimal from any specific direction. Decision space variables can be modified freely to find the optimal solution. An alternative version of this scheme would be to shuffle decision steps as needed to produce better peaking factor results. It is possible to take the decisions made in the one to one scheme and place them into an arrangement changes ordered by the steps taken and then rearrange and combine the steps as necessary to produce the minimal PPPF. An example resulting layout produced from this analysis is given in Figure 9. Beyond these schemes, diminishing amounts of information can be obtained about how the optimization method ought to operate and thus the heuristic development can be stopped here. This heuristic knowledge of the optimization method must then be implemented.

3.5 OPTIMIZATION TECHNIQUES AVAILABLE

Many stochastic optimization techniques have evolved over the last decade to solve many “black box” type problems where the underlying governing equations may be too complex to solve explicitly. These can include: tabu search, simulated annealing, genetic algorithms, among others. Many of these techniques can be implemented with fairly short development time and can often be very robust when properly adjusted to the problem of interest. Often times these techniques require only a consistent global sampling method alongside an objective function to determine the fitness of each solution. The attraction to these techniques often lies in their ability to solve such

complex real-world problems without intense manipulations in the underlying data collection techniques. GAs, for example, rely on the computational interpretation of how natural selection processes produce the most adapted biological systems for the given environment in which it exists. This technique excels in finding the neighborhood of the global optimal solution, but the end task of searching locally relies heavily on the mutation operator and thus becomes a randomized unguided approach. Tabu search is a gradient technique in which memory is collected as it performs its operations. The memory is stored in a list to obtain its optimal value. NNs or artificial neural networks (ANN) utilize a network of nodes each with their own properties specified to collect information on how the system behaves. Generally they are presented with an input / output pair that corresponds to a transformation operator. These I/O pairs represent a functional operator that acts on the input to produce the output. When invoking this operator is computationally costly, generating an ANN that effectively mimics the transformation by learning how the system works comprises the NN technique. SA is a probabilistic algorithm for global optimization problems whose inspiration comes from metallurgy where the heating of a material and successive controlled cooling reduces the defects of the metal causing it to approach a minimal internal energy. In the case of certain metals, annealing can be performed to soften the metal by reducing its overall binding energy. The analogy to optimization heuristics lay in the overall system temperature T that is slowly reduced as the process is performed (Kirkpatrick et al. 1983). Such a reduction is often exponential. Each step of the algorithm is a random permutation of the given parameters with the permutation step size reducing with system

temperature. One analogy of this technique is a bouncy ball bouncing in a mountain range. It at first has the opportunity to bounce all over the mountain range or problem domain, thus searching out the relative structure of the domain. As it bounces it loses some energy or the effective temperature of the bouncing ball reduces with each step till it finally rests in the lowest valley available to it. SA is a global optimization technique that is preferred to other techniques in specific cases. Each of these techniques can be utilized as possible optimization methods to be developed for any given problem each with their own benefits and drawbacks. The key is finding the technique that most closely finds the global optimum for the lattice with minimal time expenditure.

3.6 SA AND ADAPTIVE SIMULATED ANNEALING

Simulated annealing works by choosing system variables in the given domain, estimating the performance or "cost" of those variables, and then based on that cost and the temperature at the specified step, chooses another set of variables. System variables are generated based on predefined distributions of possible states to explore. There is also an acceptance distribution that depends on the difference between the cost value of the presently generated subspace to be explored and the last lowest subspace. Each of these distributions depends on the temperature, and thus it is crucial that the SA temperature be properly controlled. In general, an exponential decrease of the temperature is used and is called the temperature schedule. This process of calculating system variables, if repeated infinitely many times, can guarantee a global optimal solution to the given problem. The key phrase is "infinitely many times," which is not plausible. Thus the temperature schedule, along with the initial and final temperatures,

must be employed properly to approach global optima within reasonable time frames. The cost evaluation method introduced to the SA process can be thought of entirely as a "black box" process, where the SA has no knowledge of the system it is utilizing and thus must choose its system variables based solely on the input and output pairs it produces.

In order to properly implement SA, several key points are developed that govern the operation of the method. A robust SA algorithm could be built from the ground up, but there are many freely available algorithms which can be implemented with ease such as ASA. ASA is a code written by Lester Ingber that performs a simulated annealing process that is standard amongst all SA codes and is very robust and powerful. The key component of ASA that makes it such a useful tool is the ASA options available to adapt the SA algorithm to almost any global sampling application. These options allow for precise control of how the algorithm searches the domain space throughout the temperature cycle. The list of options is quite exhaustive and is available in the ASA documentation (Ingber 2007). Several of the options have been adjusted in order to take into account the large parameter space inherent in FA optimization of this nature. These will be discussed in more detail, as necessary.

3.7 OBJECTIVE FUNCTION AND GLOBAL CONSTRAINTS

With the algorithm in place, the cost function must be developed along with the constraints that determine acceptability of proposed input parameter vectors. The cost function for this work is the maximum PPPF of the FA layout that is proposed by ASA. The primary objective of this work is to minimize this PPPF. In order to obtain the

PPPF an input vector produced by ASA is transformed into a lattice physics input deck, which produces the cost estimation. This estimation is then fed back into ASA, which then decides how to produce the next layout based on these results. When choosing layouts, it is important that the layout satisfy the constraint. The constraint being applied for this work is that the average FA ^{235}U enrichment be equal to the average enrichment of the reference assembly. This should help maintain reactivity results over the FA lifetime as well as promote usage of this method in full core design. For cases that allow the Gd-pins to be inserted, an additional constraint is set in place such that the number of Gd-pins along with their Gd_2O_3 enrichment is the same. These constraints serve to develop FA layouts that are comparable to their reference designs. Additional or alternate constraints can be developed and implemented, but these are the necessary constraints for the desired solution. The constraints and cost functions are coded into the ASA algorithm so that the framework of the algorithm can be constructed.

4. LINKAGE AND FRAMEWORK

4.1 INTRODUCTION

In order to perform the optimization process, a proper framework must be developed alongside representative simulations. To build the framework of the coupling of TransLAT and ASA (TrASA), the flowchart was first developed to establish the logic that the algorithm would follow in order to properly sample the parameter domain and approach an optimal peaking value. With this flowchart in place, each of the components is coded so that data is passed properly to each task within the chart. This can be seen in Figure 10. Once established, the method can then be populated with the real FA model, and the optimization can be performed. This linkage and framework will be described further in the following sections. In general practice, it is standard to start with a reduced version of the simulation domain where the problem solution is overly obvious and then extend those initial simulations until the full system is represented.

4.2 DEVELOPING THE FRAMEWORK

Developing the flowchart starts with ASA producing an initial guess for the input vector, this vector contains integers corresponding to each of the modifications to be made. Established as a convention for this input vector, -1, 0, 1, and 2 each correspond to a Gd pin, a nominal pin, a reduced enrichment pin, and an increased enrichment pin, respectively. The nominal pin has a ^{235}U enrichment of 4.00 w/o or more generally e_{aveU} w/o if the nominal enrichment is chosen either by the user or the optimization process. Then each of the pins has enrichments reduced or increased by a specific amount e_{δ} that

is either specified in the ASA options or can be varied over any feasible range. Thus the input vector contains integers corresponding to a specific pin type being chosen by ASA. The input vector then must be translated into an input deck for the lattice neutronics code TransLAT, but it first needs to be checked against the constraints imposed. Since the constraint for this optimization is that average enrichment is conserved, a generating script is used that checks for average enrichment conservation. If the input deck does not meet the constraint requirements, then a negative cost flag is returned to ASA, the proposed layout is recorded as invalid, no neutronics calculations are performed, and a new layout is suggested. If the layout suggested by ASA passes the constraints test, an

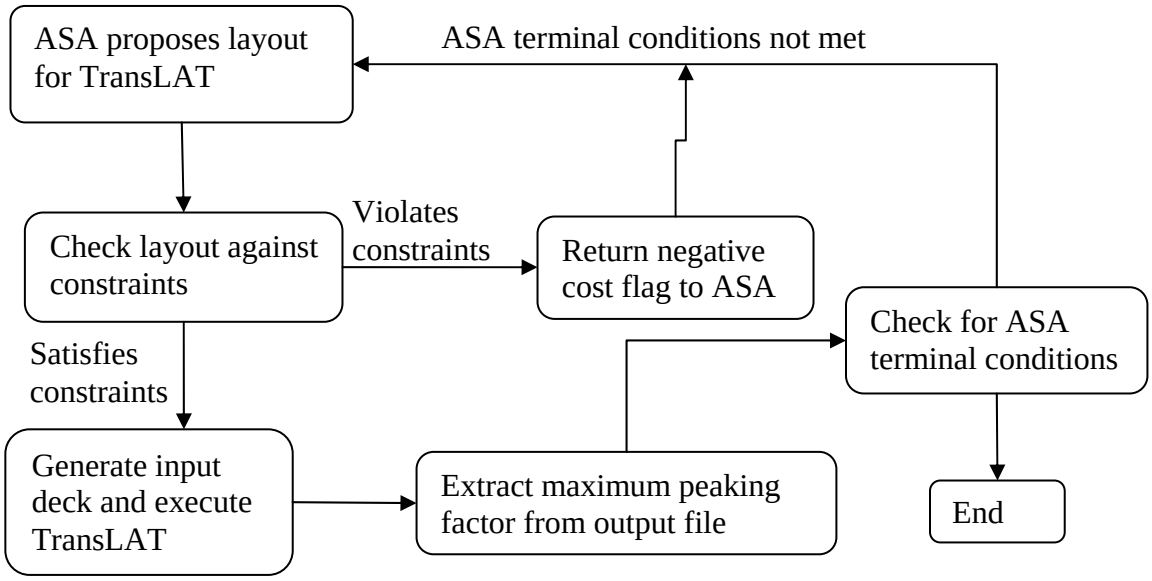

Figure 10 - ASA algorithm flowchart

input deck is generated for TransLAT by changing the lattice and geometry blocks of a nominal input deck to reflect the locations of enrichment modifications as well as

possible Gd-pin locations. This generated input deck of the acceptable layout is then run by TransLAT, which computes results such as the k-infinite, peaking factors, exposure, isotopics of the fuel, etc. The optimization cost function is then extracted from the output file and returned to ASA. When the last step is completed, ASA then performs calculations based on the previous results, random numbers, the parameter temperatures, and acceptance probabilities to generate a new layout and start the process over again. This logic is repeated until ASA approaches its optimal result. This describes the flowchart of the algorithm and is shown in Figure 10.

4.3 INPUT PARAMETERS

Most of the data needed to compute the neutronics behavior of the FA are unchanged by the optimization. These are: the geometry, material compositions (other than ^{235}U enrichment and Gd locations), system pressure and temperatures, power density, and boron concentration. For this study, the parameters that are varied pertain to the various enrichment modifications and Gd-pin placement. The user can specify: gadolinium enrichment of a Gd-pin, number of Gd-pins per FA, reduction of ^{235}U enrichment for Gd-pins, average FA ^{235}U enrichment e_{aveU}, the change in enrichment of modified fuel pins e_{δ}, and the possible pin types available for each location in the FA. Hence, a skeleton input deck is used throughout the optimization process, where only the instructions specific to ^{235}U enrichment and Gd-pin location are to be generated at each trial. This list of parameters is referred to as the input vector, which is an ordered vector of integers with each component corresponding to each of the specific parameters used in the optimization process. Parameters of the input vector are as listed in Table 3.

Across the top row are the components of the input vector, and the second row contains typical values or ranges of values that each component may take. While most of the parameters remain as they are, a few are translated into their true meaning. Most notable

Table 3 - Input vector of parameters with sample possible values and ranges

e_{Gd}	e_{GdU}	n_{Gd}	e_{aveU}	e_{δ}	32 pin locations
(0,6)	(0,3.75)	(0,20)	[4,4.5]	[0,40]	(-1,0,1,2)
pin types	0=std pin	1=e_{aveU}-e_{δ}	2=e_{aveU}+e_{δ}	-1=Gd pin	

of these is the e_{δ} parameter, which is an integer in the input vector. Values for this parameter are allowed to vary from zero to any specified value less than 90. This integer is then transformed by division by one hundred so that the decimal point moves two places to the left. For instance a value of e_{δ} of 25 would correspond to 0.25 w/o ^{235}U enrichment change. Another such parameter that is transformed is the e_{aveU}. This is another integer parameter that is transformed into decimal form by division of one hundred. This value is then added to four to give the average FA enrichment desired. This parameter is not always varied as described in the case studies but can be if desired by the user. The last parameter that is modified in the code is the number of Gd-pins, n_{Gd}. Since simulations are being performed in $1/8^{th}$ symmetry and n_{Gd} is the number of Gd-pins in the whole fuel assembly, a system of verifying that the number of Gd-pins suggested by ASA corresponds to n_{Gd} number of Gd-pins. A weighting vector is applied as seen in Figure 11, where the weighting factor of pins along the diagonal edge as well

as the bottom edge are replicated only four times when expanding to the full FA, while the rest of the pins are replicated eight times. TrASA uses this weighting vector to check

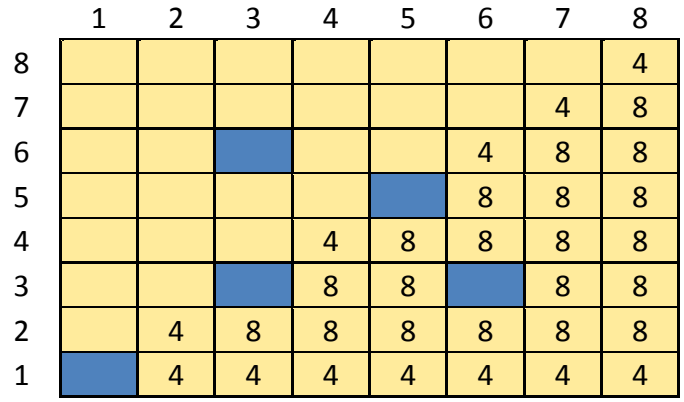

Figure 11 - Visualization of the weight vector applied to the constraints

that the n_{Gd} parameter is satisfied as well as to check that the average enrichment constraints are maintained. This input vector allows for the generation of the necessary input decks used to perform simulations to subsequently obtain the peaking factor for the FA.

4.4 INITIAL SIMULATIONS

With the framework of the method in place, some initial simulations were performed to test the framework and establish that it produces intuitive results. The smallest feasible system that maintains relevance to the baseline is a 4x4 FA with one water hole in one of the four interior locations. This FA can be thought of as a portion of the full 15x15 FA where the fuel pin to water hole ratio is similar. With this 4x4

model in place, the algorithm's logic was tested. A version of TrASA was built for this system with ASA generating the enrichment values for the fifteen fuel pins and then evaluating the resulting peaking factor of the 4x4 system. This optimization runs in a very short amount of time since the number of parameters to vary is very limited. Although the link to the actual fuel assembly is weakened somewhat, a 3x3 system was built for the purpose of experimenting with the options available in the ASA code. Selection of the water hole locations in each of these systems can be freely chosen since their correlation to real sections of the FA is almost completely lost. The one correlation that does remain is the behavior of how a fuel pin interacts with neighboring water holes, making the results useful in adapting ASA to the solution space. This behavior is the essence of the optimizations, since the water holes contribute the most to perturbations experienced in the FA flux. If the FA were only made of fuel pins, the peaking factor map would be completely flat with an infinite lattice assumption in place.

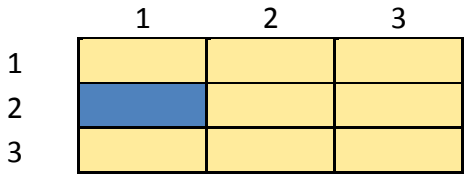

Figure 12 - TrASA 3x3 baseline FA layout with one water hole

Although the 3x3 system is not intuitively connected to the real FA, its results are interesting in that the proposed best layout from ASA reflects what an engineer would

arrive at when trying to achieve the same goal intuitively. The water hole location was selected merely as convention because the solution to the minimal peaking factor problem can be intuitively found. The baseline FA for TrASA-3x3 is as shown in Figure 12, where the water hole is in row two and column one. Resulting modifications as well as peaking factor data produced by TrASA-3x3 are given in Figure 13. The enrichment

Enrichment Layout

	1	2	3
1	3.65	4.00	4.35
2		3.65	4.35
3	3.65	4.00	4.35

Pin Power Values

	1	2	3
1	1.130	1.120	1.126
2		1.076	1.131
3	1.130	1.120	1.126

Figure 13 - Layout and Pin Power Results from TrASA-3x3 optimization

delta range was set to [10,35] for this simulation. It is not necessary to analyze this system further due to its disconnection with the real FA and since the model is developed to confirm that TrASA produces results as expected on a simple system. As for the 4x4 system, it too produces a layout that seems fairly intuitive. The layout and resulting peaking factor are shown in Figure 14. It is not intuitively obvious why in row two column one there is a reduction in ^{235}U enrichment, but all of the cells that are face adjacent to the water hole are reduced which is intuitive. This illustrates how one step away from the simplest model introduces the need for a method like ASA. Multiple

Enrichment Layout

	1	2	3	4
1	4.25	4.25	4.25	4.25
2	3.75	4.00	4.00	4.00
3	4.00	3.75		3.75
4	4.25	4.00	3.75	3.75

Pin Power Values

	1	2	3	4
1	1.061	1.069	1.081	1.080
2	0.988	1.054	1.089	1.072
3	1.046	1.046		1.074
4	1.087	1.077	1.076	1.059

Figure 14 - TrASA-4x4 Enrichment Layout and Pin Power output

layouts can be produced at this level to give the optimal minimum peaking factor, allowing for selection of the "best" layout to satisfy other possible needs the designer might have. With these illustrations in place, it is then possible to expand simulations to the full 15x15 FA model and begin analysis of those results.

5. CASE STUDIES

5.1 CASE STUDIES

Obtaining meaningful results from TrASA requires developing representative case studies to be performed and then tuning the ASA options to that problem so that ASA is truly "adapted" to the lattice physics code. Several iterations in developing cases, analyzing those cases, and then modifying the cases to best represent the methodology is an integral part of the optimization process. Two classes of cases are presented here: the optimization of a 15x15 UOX FA without any Gd poison and the optimization of a 15x15 UOX FA with gadolinium pins. Although these are two separate optimizations to perform, TrASA is a package that can run these cases indifferently, based on the general input parameter vector developed in this work. For instance, to run a non Gd-bearing case, all the Gd parameters are set to zero and thus limit TrASA to compute a UOX case. Each of these classes was studied and is analyzed here.

5.2 DEVELOPING THE CASE STUDIES

Stochastic methods like ASA require development of a set of cases to be run and analyzed in order to verify that the optimization process runs as expected as well as to determine the optimum set of parameters. In general, the procedure for developing cases begins with fixing many of the parameters and allowing the optimization to search a small subspace of the whole domain. Although this might not give the best results, it allows the user to verify that the process is running as expected. With satisfactory

results found additional parameters can be varied allowing the code more and more freedom to search the domain. Each additional parameter variation that is allowed introduces both flexibility and difficulty. The addition of parameter variations makes it sometimes more difficult to compare to the baseline reference case. Despite this, the added flexibility allows for more results to be produced and possibly a better optimal solution. This methodology helps build new intuition on how the various parameters should be arranged and chosen such that the optimal solution is found.

5.3 UOX CASES

The optimization cases with only uranium dioxide fuel are a subset of the larger optimization class of UOX fuels with some pins bearing gadolinium poison. It is thus a simpler problem to solve for sampling algorithms such as ASA since it requires less sampling of the space. The initial case that was run sets all of the values in the input

Table 4 - Case descriptions for UOX (non-Gd) optimizations

	e_{Gd}	e_{GdU}	n_{Gd}	e_{aveU}	e_{δ}	pins used	description	resulting pppf	types
Case 1	0	0	0	4	0.17	(0,1,2)	initial optimization	1.092	0=std pin
Case 2	0	0	0	4	[0,0.40]	(0,1,2)	variation in e_{δ}	1.092	1=e_{aveU}-e_{δ}
Case 3	0	0	0	[4,4.5]	0.17	(0,1,2)	variation in e_{aveU}	1.092	2=e_{aveU}+e_{δ}
Case 4	0	0	0	[4,4.5]	[0,0.40]	(0,1,2)	variation in both	N/A	

vector to constants and only manipulates the enrichment map of the fuel pins. It maintains a constant average enrichment and uranium enrichment delta, and searches that space. This input vector can be seen in Table 3 where all of the UOX cases are listed with their respective variable ranges and descriptions. The four cases listed are the UOX representative cases. The variation ranges allowed on each of the parameters have been selected as per assumptions made from literature and industry standards. The first case, case 1, is the initial optimization which can also serve as a baseline from which the rest of the cases can be compared. Case 1 produces a PPPF of 1.092 which is a 2.5% reduction of the PPPF from the baseline results. A visualization of the peaking factors that ASA finds as it progresses through the optimization can be seen in Figure 15. The cost temperature of this case can be seen in Figure 16. These two plots show how ASA samples the space and approaches its minimum PPPF. Each peak that can be seen in Figure 15 represent ASA trying to bounce out of any local optimal values that have been found. The temperature schedule is somewhat aggressive but the method must run in a decent amount of time and thus the cost temperature is reduced as shown. The next case, case 2, allows for variation of the uranium enrichment delta parameter, e_δ. In this case the average enrichment remains constant and the parameter range as given in Table 4 allow enrichments as low as 3.60 w/o ^{235}U and as high as 4.40 w/o ^{235}U. The resulting PPPF of this simulation was also 1.092. This is because the enrichment delta chosen for case one was chosen in the optimal range of that parameter. This result confirms that the two cases converge to the same parameter domain showing the variation in uranium enrichment deltas produces accurate results.

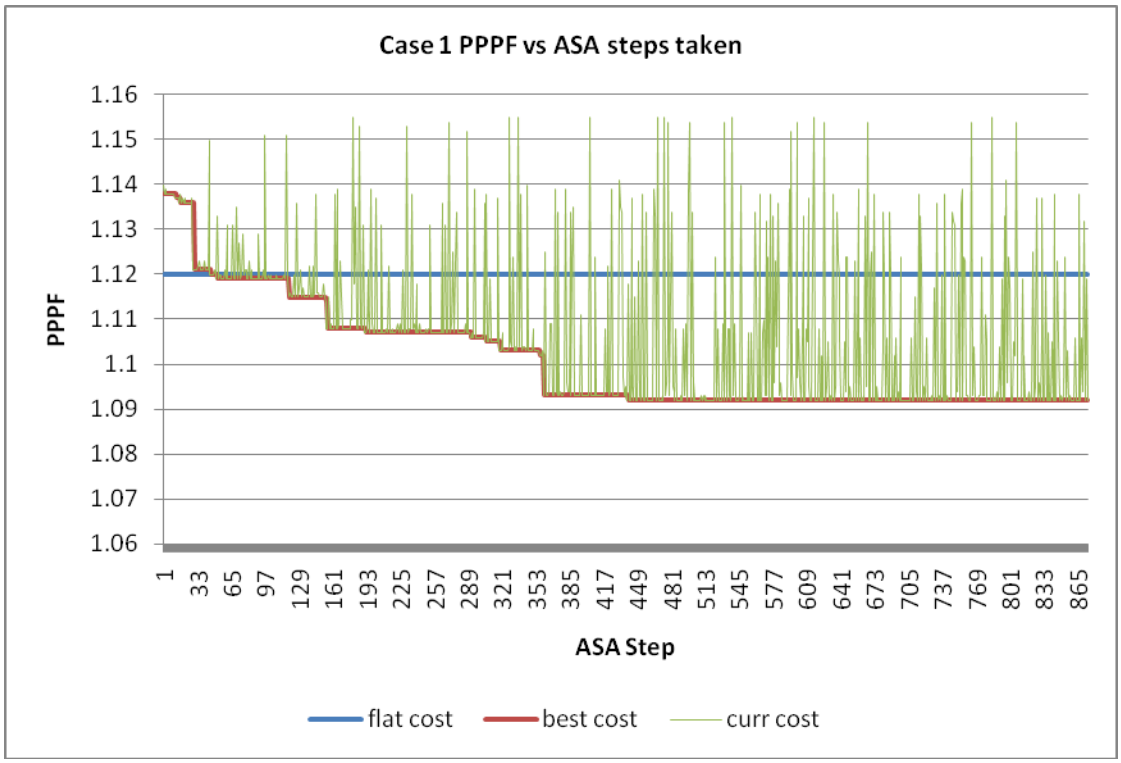

Figure 15 - Cost estimation for case 1 as ASA perturbs the layouts to minimize the PPPF

The next case, case 3, studies how the average uranium enrichment affects the PPPF of the FA. This case may be a bit contrived and requires that baseline references be produced at the conclusion of the optimization. That is to say if the optimization finds that an average FA ^{235}U enrichment is 4.2 w/o then baseline results should be taken from a flat enrichment FA with all pins at 4.2 w/o ^{235}U. The resulting PPPF from this case is again 1.092 with an average enrichment of 4.01 w/o. The trend produced in

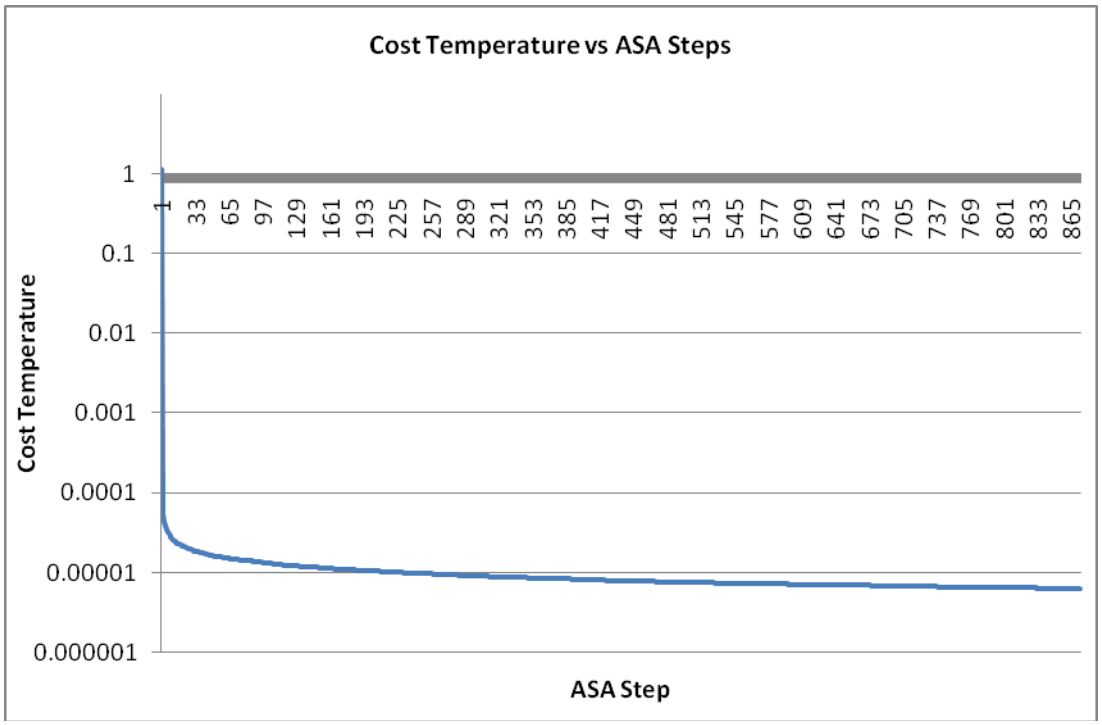

Figure 16 - Cost temperature as a function of each step taken by ASA

this optimization agrees with the intuition that minimizing the total average ^{235}U enrichment will result in the lowest peaking factor of the FA. Despite this, case 3 verifies that the optimization produces the correct trend. In order for this case to really make sense or be of some value the objective function would need to be modified so that the positive effects of higher average enrichment were rewarded. The last case, case 4, in this class of cases performs all UOX variations. This can be an interesting case but it will not be performed or analyzed in this study. Since the parameter space for these optimizations is already very large, allowing TrASA to perform this optimization does

not yield as good of results as the previous cases in any reasonable amount of time. It is best as will be shown in later sections to guide TrASA into the optimal space with knowledge of the system thus reducing erroneous solutions. Additionally, each of the parameters have been studied independently each trending towards the same optimal region invalidating the necessity of this case. Results from these cases as well as further analysis will follow in later sections.

5.4 UOX WITH GADOLINIUM CASES

The other class of optimization contains the gadolinium cases which are in a wider space than that of the UOX cases. Allowing Gd-pins to be inserted into the FA increases the levels of complexity, which in turn makes the solution more difficult to find, and requires more simulations. Although three more parameters must be used to specify these cases, number of Gd-pins n_{Gd}, uranium enrichment in the Gd-pins e_{GdU}, and natural Gd enrichment in Gd-pins e_{Gd}, most of the time these additional parameters will be fixed so that they can be more easily related back to the baseline design. If these parameters were varied, a new baseline would need to be defined for those cases, e.g., the baseline FA, as described in section 2, considered here contains 20 Gd-pins with a 6 w/o enrichment in Gd_2O_3 and a slightly reduced ^{235}U enrichment (3.75 w/o) producing a peaking factor of 1.173. Our framework can allow these to be also changed in TrASA but there would be no grounds to compare these results with the selected baseline (industry standard) FA with Gd-pin. Hence, our constraints are that the number of Gd-pins is fixed, their enrichment in Gd is not varied, and their enrichment in uranium is not varied.

The first case that was built can be considered the first step away from the baseline FA with Gd-bearing pins. This case is case 5 of Table 5 where the Gd-pin

Table 5 - Case study descriptions for the UOX with Gd optimizations

	e_{Gd}	e_{Gdu}	n_{Gd}	e_{aveU}	e_{δ}	pins available	description	resulting pppf	types
Case 5	6	3.75	20	4	[0,0.35]	(0,1,2)	gd loc fixed per baseline	1.151	0=std pin
Case 6	6	3.75	20	4	[0,0.35]	(-1,0,1,2)	all variations	1.162	$1=e_{aveU}-e_{\delta}$
Case 7	6	3.75	20	4	0	(-1,0)	opt gd locs	1.170	$2=e_{aveU}+e_{\delta}$
Case 8	6	3.75	20	4	[.10,.25]	(-1,0,1,2)	restrict gd locs	1.149	-1=Gd pin
Case 9	6	3.75	20	4	[.10,.25]	(-1,0,1,2)	restrict gd and UOX locs	1.147	

locations of the baseline layout are fixed and the remaining fuel pin locations have their ^{235}U content modified with a variable delta. The range for the change in enrichment is from -0.35 to 0.35 w/o ^{235}U. The peaking factor produced for this case is 1.151 which compares to the 1.170 PPPF of the baseline FA. With this initial case developed and analyzed further cases can be developed to test the variations of the parameters to try to obtain even lower peaking factors.

The next case is case 6 as in Table 5 where the e_{δ} is varied over the same range and all locations can be changed. This parameter could be varied over any range but for consistency will remain the same range as the previous case. The main alteration in this case is to allow movement of the Gd-pins and examine the effects this has on the output. The PPPF produced here is 1.162 which is worse than the previous case. The layout

produced here would most certainly not be practical since it would increase the cost of fabrication of the FA with little returned value. These results do not follow the intuition of the researchers since increasing the parameter space in most methods still allows for the optimal solution to be found. Due to the size of the parameter space in this case and the nature of the SA algorithm being used, and probably of all SA algorithms, it is actually best to try to introduce as much *a priori* knowledge into the system and try to help along the SA code as much as possible. Introduction of beforehand knowledge of the system must be applied with caution however, since too many restrictions may be introduced, disallowing the optimization from sampling the optimal space and possibly restricting the search to a too narrow domain. The following cases, 7 through 9, attempt to guide TrASA towards an optimal solution by imposing additional constraints.

One way to guide TrASA properly to the optimal search space is to find the optimal set of Gd-pin locations and then only allow those locations in subsequent cases. The next case that follows, which is case 7 as given in Table 5, searches for the optimal Gd-pin locations. In this case only the Gd-pins are allowed to be inserted making the need for uranium enrichment variations unnecessary. This is a comparatively small variational space to search and thus the case runs very quickly as compared to the other cases. It is important to note here that it is sometimes best to penalize usage of certain locations for Gd-pins. There are several phenomena that contribute to making this decision and ultimately decisions of this nature are at the behest of the designer and depend on the specific implementation. Locations of fuel pins along the outside edge of the FA as well as the locations that are both face and corner adjacent to the IT are often

times either not allowed or penalized when Gd-pins are inserted there. Usage of Gd-pins in the locations along the periphery of the FA greatly disturb the flux on the edge of the FA which is adjacent to, in general, at least once burned FAs in power reactors. Since simulations are performed here under infinite lattice assumptions, they may not exhibit the issues relevant to core level peaking factors, thus it is often preferred not to place Gd pins at the FA periphery. As for the locations around the IT, usage of Gd-pins in these locations may disturb the readings produced by the IT, a situation to be avoided for the purpose of flux mapping. For these reasons, the aforementioned locations can be disallowed or penalized depending on the approach taken in the code. The restriction applied to case 7 is that none of the periphery locations are allowed to contain Gd-pins and the locations that are face adjacent to the IT are not allowed. The corner adjacent location can be allowed as per these assumptions since such a high PPPF has occurred there in previous simulations. Allowance of this location can be argued either way but for this analysis it will be allowed for the reasons stated above. This constraint can be seen in Figure 17. With this knowledge about the FA implemented into the case parameters, the optimization was performed. Since the location in the (8,8) position is not allowed and the peaking factor often resides in that location, information that the code gains from manipulating the Gd-pin locations is limited. Despite this, case 7

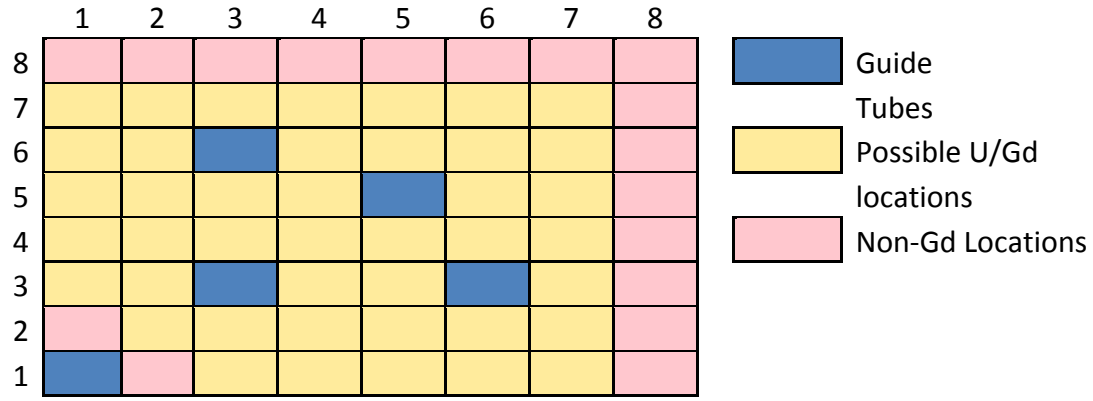

Figure 17 – Gd-pin restrictions as used in cases seven, eight, and nine as adapted from Yilmaz et al. (2006)

produces a layout with a PPPF of 1.170 which is not much of an improvement over the baseline result of 1.173. As an inherent limitation, TrASA produces families of optimal results due to both truncation error within TransLAT and the limitation in TrASA of using only three specified enrichment values. A full spectrum of enrichments could be allowed but would be unrealistic and costly to manufacture. If all parameters were treated as continuous it would be more likely that one solution would be found but that is not the case. These results however prove beneficial in developing the cases that follow.

An optimization like case 8 can be used to produce optimal layouts that place Gd-pins in a set of optimal Gd-pin locations. Combined with results from case 7, this set of locations can be used to constrain the optimization so that Gd-pins are only inserted in these locations as given in Figure 18. That is to say that, in any of the specified locations, it is possible to insert a pin of any type including Gd-pins while in the rest of the locations only nominal, reduced or increased enrichment pins will be available. This

keeps the code from suggesting layouts that have Gd-pins in the “wrong” locations. Case 8 optimizes with this restriction in place. The PPPF of this simulation is 1.149.

	1	2	3	4	5	6	7	8
8								4
7							Gd	4
6						Gd	4	4
5						4	Gd	4
4				Gd	4	Gd	4	4
3				4	4		Gd	4
2		Gd	4	4	4	4	4	4
1		4	Gd	4	Gd	4	Gd	4

Figure 18 - Optimal Gd-pin locations used for setting restrictions in Case 8 optimization

This is an improvement over the previous cases and is a reduction that should be expected. The goal here is that the parameter variations are properly tuned to produce the best result possible within a reasonable amount of time. For this reason a simulation of TrASA was performed similar to case 6 where the enrichment delta parameter is varied. The corresponding peaking factor as a function of the enrichment delta parameter is generated from a simulation like case 6 and is plotted in Figure 19.

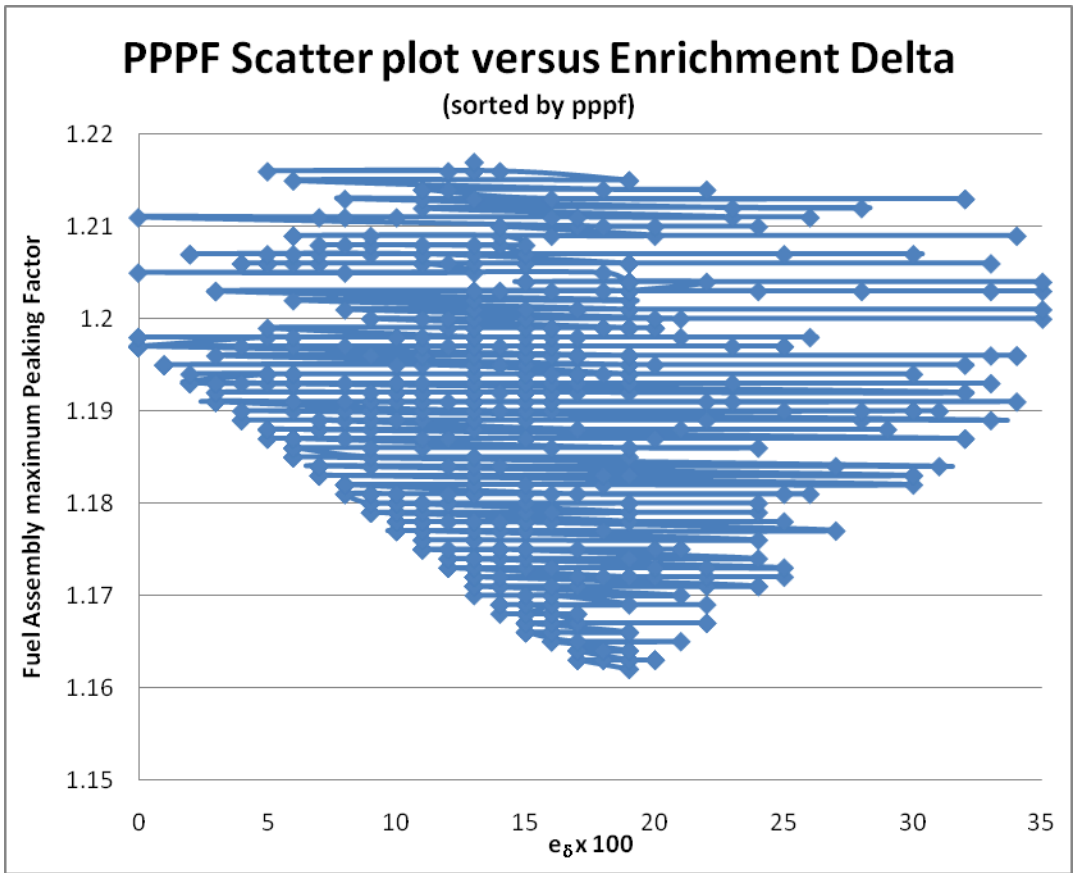

Figure 19 - Scatter plot showing peaking factors produced as a function of enrichment delta

This plot shows a scatter plot of the data and is sorted by peaking factor produced to show how the code converges to the optimal delta. This leads to narrowing this parameter's range to the optimal range. It is feasible that with an infinite amount of time all cases could converge to the same solution. The only thing that makes this case better is that the options were tuned more accurately to the problem domain and was able to find a more optimal solution in the reasonable time frame. In order to implement more knowledge into the system, one further step can be taken in constraining the

optimization space. This next step is similar to the constraints applied in case 8 but pertains to the uranium enrichment modifications of the fuel pin locations. The same method can be applied as before where the fuel pin modifications that have high frequency in previous studies can be used. This is illustrated in Figure 20 where each cell contains the best pin types to be inserted in each location. To develop these

	1	2	3	4	5	6	7	8
8								1
7							-1,0	0,1
6						-1,0,1,2	1,2	0,1,2
5						1,2	0,1,2	0,1,2
4				-1	0,1	1	1,2	1,2
3				0,1	0,1		-1	2
2		-1,0,1	0,1	0,1,2	0,1	0,1	0,1,2	0,1
1		1,2	0,1	0,1,2	0,1,2	0,1,2	1,2	0,1,2

Figure 20 - Visualization of restrictions used for case 9 where each number represents the allowed pin types at each location

constraints, the best layouts from previously run case studies were listed in a spreadsheet. Then for each location the pins that are usually inserted for each of the 'optimal' layouts were allowed. That is to say that for a specific location if the optimization generally selected either a nominally enriched fuel pin or a decreased enrichment fuel pin then it is not necessary to allow any other pin types since they will lead to higher peaking factors. This was done for each of the locations in the FA which designates case nine. Case 9 produces a peaking factor of 1.147 which is a further improvement over case 8. These cases serve to develop the method of applying the

simulated annealing approach to FA optimization. Several iterations of this methodology should be expected to properly guide TrASA into the optimal search space.

5.5 UOX DETAILED RESULTS

Each of the cases above produces resulting layouts that should be analyzed further. The optimizations of this class often find multiple FA layouts that all produce the same 'optimal' peaking factor result. These layouts require analysis to determine the layout that is best to use in a given application. All three of the cases run give the same optimal peaking factor of 1.092 but produce numerous layouts that give this value. Case 2 gives a few layouts with uranium enrichment deltas of 0.17 w/o and 0.18 w/o as optimal values for this parameter, while the third case gives average uranium enrichment values from 4.00 w/o ^{235}U to 4.4 w/o ^{235}U. To pick the best layout to use one could use several metrics. Depending on engineering needs the designer could choose the layout with the most or least number of enrichment changes to have the most or least modified layout. These two fringes of the family of layouts can be expected to reduce cost, specification error, and manufacturing error. Cost could be reduced by limiting the number of differently enriched pins. Specification and manufacturing error can be reduced because the layouts are somewhat simpler reducing the possibility of human error. Alternatively the layout with the best k_{inf} performance could be chosen. Yet still another method could be to look at the changes that have been made to each location over all the optimal layouts and see if those locations are preferable to other locations.

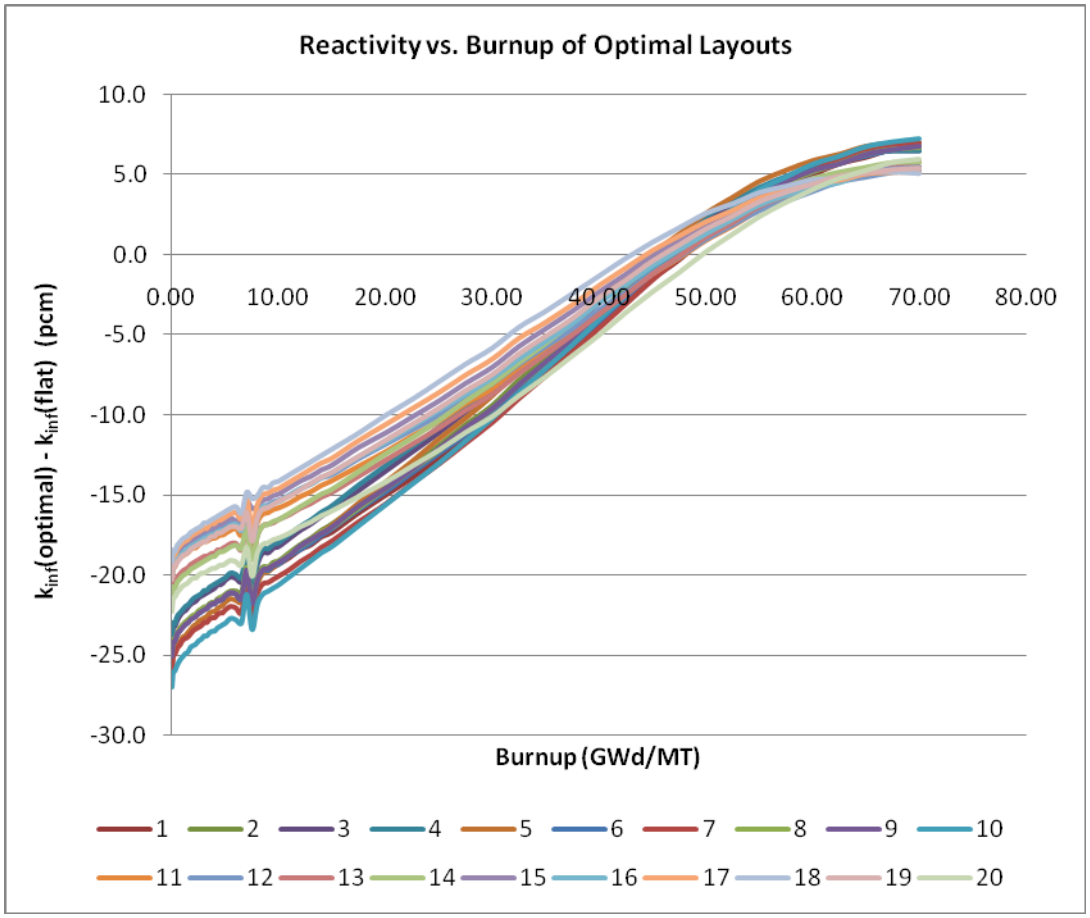

Figure 21 - FA reactivity compared to baseline FA results for twenty optimal layouts produced with the same peaking factor

This is motivated by the fact that many of the layouts produced fall into classes where one location has the same change made. That is to say a class of these layouts would all have possibly the reduced enrichment uranium pin inserted in the same location where the other class might have just the nominally enriched pin inserted in that same location.

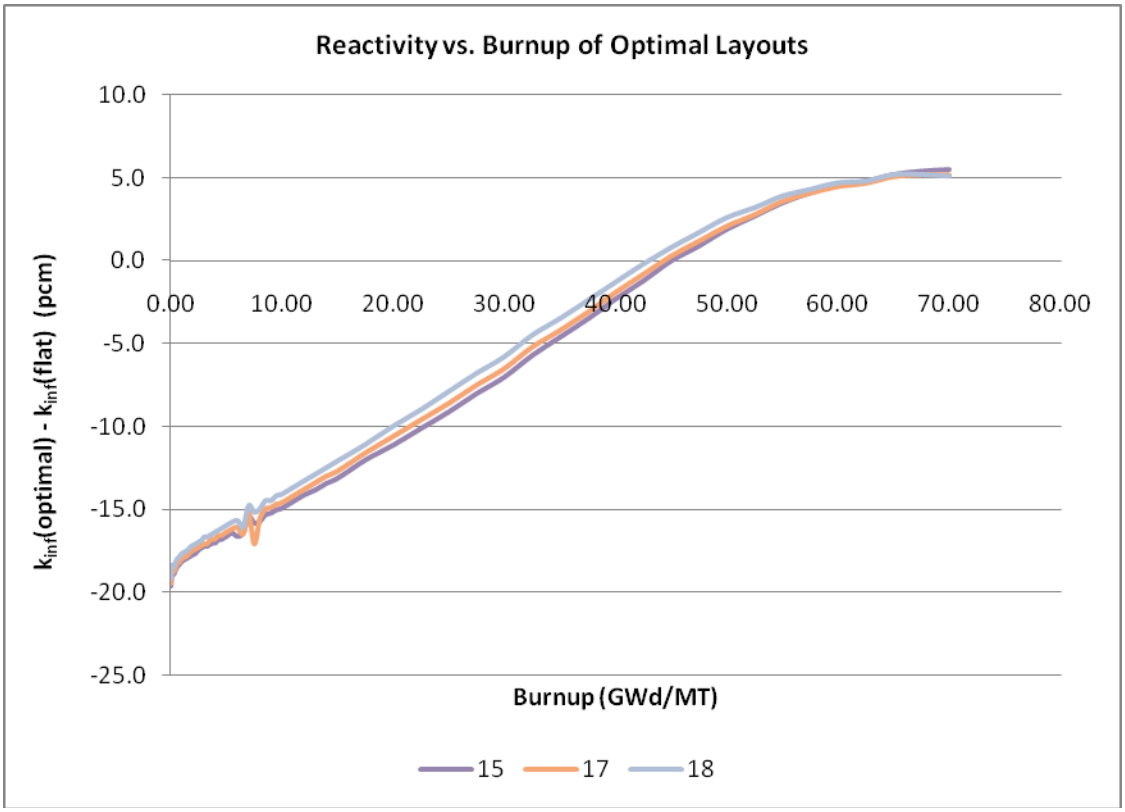

Figure 22 - Reactivity vs Burnup for selected optimal layouts

All together there are 169 different layouts produced with the same peaking factor. In order to narrow the field for possible candidates some filter must be applied to choose the best layout. Appropriate filters for these layouts are not fully developed as of this project and thus the aforementioned strategies are employed for selecting the most desirable layouts. Of the layouts produced, a group of them were chosen based on the number of pin cell alterations. This subset of layouts contains those that had both the highest number of fuel pin changes as well as the lowest number of changes. Another way of expressing this would be to count the number of fuel pins in each layout that are the average ^{235}U enrichment and use the layouts with the highest and lowest number of

these pins. There are several layouts with as many as fifteen nominally enriched fuel pins and then quite a few with as few as six. These numbers are counting only the number of these fuel pins contained in the $1/8^{th}$ assembly layout specification. To count them in the full FA the weighting factors must be taken into account as it applies to where the fuel pins are located. With the field of candidate layouts reduced, several of the other methods of looking for the most desirable layout can be employed. Since FA reactivity is a major indicator of FA performance, those results will be analyzed. Each of the layouts is numbered in no particular order but merely for convention. Figure 21 shows a plot of the reactivity with respect to burnup for each of the twenty optimal layouts produced. Reactivity in each case is calculated as the difference between k-infinite of the FA layout and the k-infinite of the baseline FA times a scaling factor to cast the values into a familiar unit of measure. Most of the twenty cases have very similar reactivity plots with respect to burnup. FA's that have the least negative reactivity would be preferable in any design and thus the list of optimal layouts can then be reduced further to possibly three layouts that all have the least reactivity over the time period of interest. Those layouts are 15, 17, and 18 and their reactivities are shown in Figure 22. Selection of the best of these three then is left to the designer to pick which

	1	2	3	4	5	6	7	8
8								4.00
7							3.83	3.83
6						3.83	4.00	4.00
5						4.00	4.17	4.00
4				3.83	3.83	3.83	4.17	4.00
3				3.83	3.83		4.00	4.00
2		4.00	4.00	4.17	4.00	4.00	4.17	4.17
1		4.00	4.17	4.17	4.00	4.17	4.17	3.83

Figure 23 - Optimal layout 15 produced with peaking factor in red

layout should be used. It is interesting to note that the layouts chosen based on reactivity are all in the lowest number of changes. The optimal layouts can be visualized as in Figure 23, Figure 24, and Figure 25. Looking at the layouts produced yields some assurances that relate to engineering intuition and some surprises. TrASA has found a central core of fuel pins that are always reduced in uranium enrichment. It also suggests that no locations that are face adjacent to water holes have increased enrichment. Both of these findings follow with standard physical intuition. The locations that seem to go against intuition are the corner adjacent to water hole locations. Several times an increased enrichment pin can be inserted in these locations to obtain the minimal peaking factor observed. If one were to base an enrichment grading strategy on these results, the first need would be to establish the core locations that have reduced enrichment and then spread out the increased enrichment pins throughout the lowest peaking factor locations. These results could be analyzed further but that analysis might

not yield anything beneficial to the study here due to the infinite lattice assumptions inherent in these simulations.

	1	2	3	4	5	6	7	8
8								3.83
7							3.83	3.83
6						4.00	4.00	4.00
5						4.00	4.17	4.17
4				3.83	3.83	3.83	4.00	3.83
3				3.83	3.83		4.00	4.17
2		4.00	4.00	4.17	4.17	4.00	4.17	4.17
1		4.00	4.17	4.00	4.17	4.00	4.00	3.83

Figure 24 - Optimal layout 17 produced with peaking factor in red

	1	2	3	4	5	6	7	8
8								3.83
7							3.83	3.83
6						4.00	4.00	4.00
5						4.00	4.17	3.83
4				3.83	3.83	3.83	4.00	4.17
3				3.83	3.83		4.00	4.17
2		4.00	4.00	4.17	4.17	4.00	4.17	4.17
1		4.00	4.17	4.00	4.17	4.00	4.00	3.83

Figure 25 - Optimal layout 18 produced with peaking factor in red

5.6 UOX WITH GADOLINIUM DETAILED RESULTS

Cases of this class produce fewer layouts with the same peaking factor and often times produce only one or two layouts with the lowest peaking factor found. Therefore it is less of an arduous task to analyze these results as there is less decision making involved in finding the best suited layout. As an effect of the normalization method used in TransLAT peaking factors produced from this class generally are not quite as low as the previous class that does not include Gd-pins. Despite this, the method does produce peaking factor reductions that compare well to these cases' baseline fuel assembly results. Due to the gadolinium pin restraints imposed, where several of the locations are less than favorable for Gd-pins to be inserted, peaking factors are not the lowest that have been experienced but the constraint is a necessary addition to exemplify how this method can be modified to reflect real world FA design constraints. Since the various

	1	2	3	4	5	6	7	8
8								4
7							Gd	4
6						4	4	4
5						4	4	4
4				Gd	4	4	4	4
3				4	4		Gd	4
2		Gd	4	4	4	4	4	4
1		4	4	4	4	4	4	4

Figure 26 - Optimal Gd-pin layout produced from case 7

cases are more steps along a path towards the best implementation of TrASA than they are independent stand alone solutions, case 9 and case 7 are the two cases that best exemplify the true results of TrASA. For case seven, there are two layouts that are produced based on whether or not the location corner adjacent to the IT location is allowed to TrASA. As stated before, this location was allowed in later cases merely as a convention. The optimal Gd-pin locations with this location allowed are given in Figure 26. These optimal locations were then implemented into later cases, as described in

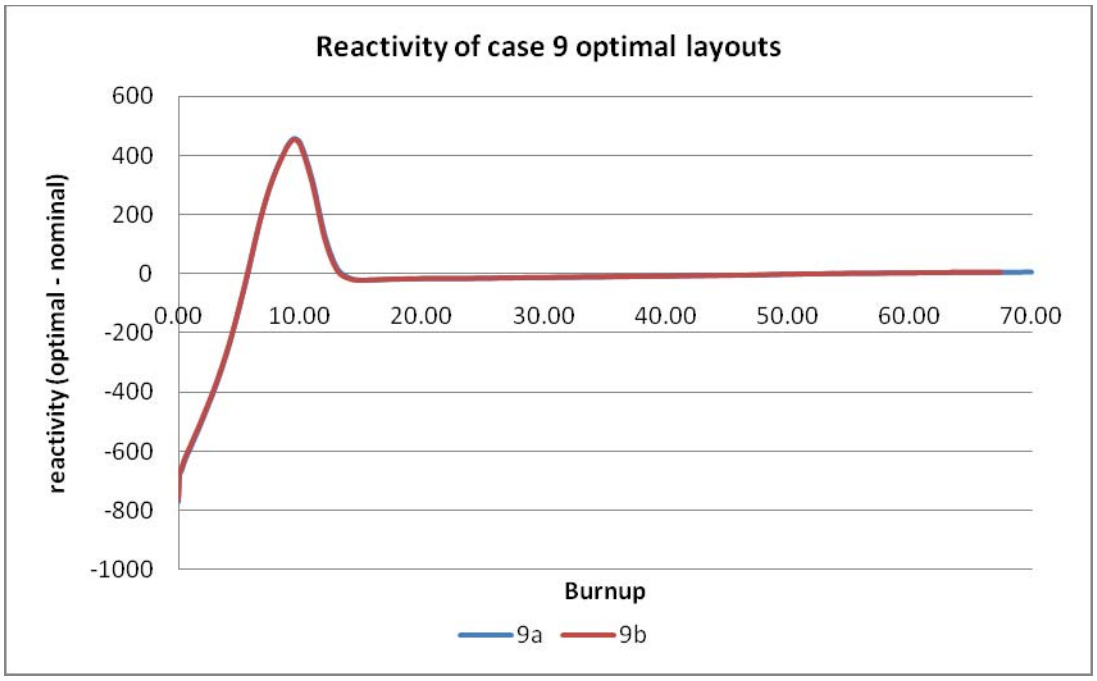

Figure 27 - Reactivity performance of both layouts produced from case 9 as compared to nominal Gd-pin layout

the previous sections, which lead to case 9. For case 9, there were two layouts produced with the same peaking factor which were very similar. Case nine layouts have reactivity performances as shown in Figure 27. The reactivity for the burnup period is almost

	1	2	3	4	5	6	7	8
8								3.87
7							Gd	4.00
6						3.87	4.13	3.87
5						3.87	4.00	4.13
4				Gd	4.00	3.87	4.13	3.87
3				4.00	3.87		Gd	4.13
2		Gd	3.87	4.13	4.00	4.00	4.13	4.00
1		4.13	4.00	4.13	4.00	4.00	4.13	3.87

Figure 28 - Case 9a optimal fuel pin layout with peaking factor marked in red

identical for both layouts and shows the gadolinium burnup period where the two main isotopes ^{155}Gd and ^{157}Gd burn out allowing the fresh fuel in the Gd-pins to contribute to the reactivity of the FA. Layouts for this case are as shown in Figure 28 and Figure 29, with the peaking factor maps of these optimal layouts shown in Figure 30 and Figure 31. Although these layouts do produce a negative reactivity when compared to the baseline FA for a period of time in the burnup period, careful examination of Figure 27 will show that the negative reactivity produced is for a short period of time. The reactivity then becomes positive as the gadolinium is burned out and then stabilizes. This layout should be implementable in a modern PWR if the boron concentrations are adjusted to match the negative reactivity introduced so that sustained power operation could be maintained.

	1	2	3	4	5	6	7	8
8								3.87
7							Gd	4.00
6						3.87	4.13	4.13
5						3.87	4.00	4.00
4				Gd	4.00	3.87	4.13	3.87
3				4.00	3.87		Gd	4.13
2		Gd	4.00	4.13	4.00	4.00	4.13	3.87
1		4.13	4.00	4.13	4.00	4.00	3.87	3.87

Figure 29 - Case 9b optimal fuel pin layout with peaking factor marked in red

	1	2	3	4	5	6	7	8
8								1.071
7							0.447	1.052
6						1.091	1.080	1.066
5						1.146	1.110	1.144
4				0.454	1.147	1.136	1.104	1.075
3				1.115	1.134		0.452	1.085
2		0.442	1.061	1.141	1.139	1.144	1.098	1.098
1		1.022	1.067	1.133	1.125	1.124	1.128	1.091

Figure 30 - Case 9a pin power results at burnup zero with Gd-pin locations in green and maximal peaking factor in red

	1	2	3	4	5	6	7	8
8								1.068
7							0.446	1.049
6						1.090	1.078	1.112
5						1.146	1.110	1.119
4				0.454	1.147	1.136	1.104	1.076
3				1.114	1.134		0.452	1.087
2		0.442	1.084	1.140	1.139	1.146	1.101	1.077
1		1.021	1.065	1.131	1.125	1.127	1.083	1.096

Figure 31 - Case 9b pin power results at burnup zero with Gd-pin locations in green and maximal peaking factor in red

6. CONCLUSIONS AND FUTURE WORK

6.1 IN CONCLUSION

The implementation of ASA to FA optimization has been completed with favorable results. The purpose of this work is to develop a simulated annealing approach to FA optimization that can produce optimal FA layouts for the types of FA, with and without burnable poisons. This method successfully reduces the peaking factors with respect to the baseline FA references. Reductions in peaking factors, however small, are useful for investigating ways to produce better performance characteristics. Each of the cases produced in this work examine the steps necessary to develop a feasible method that produces optimal results within reasonable time constraints. This work, of course, is part of a bigger whole aimed at operating commercial nuclear power plants with their fullest potential maximized. The larger body of work that this fits into takes into account core level optimization as well as multi cycle analysis. Connection of this method to the larger body of work is necessary to produce more feasible results.

6.2 CONNECTING TO IN-CORE OPTIMIZATION

It is important to note that this work is limited mostly by the necessary infinite lattice assumption. In order to remove this assumption, some knowledge of where the FA might be placed in the core is necessary. A complete optimization process would include multi cycle analysis, core level optimization, and this FA optimization work. Connecting this work to the core level optimization requires prior knowledge of the neighboring FA burnup characteristics, which are not available at this time. For this

reason the infinite lattice assumption was allowed to persist through all the simulations performed. This artificial separation of the FA level optimization from core level optimization must be removed at some point for this work to move forward.

6.3 CONCLUSIONS

The developed method TrASA successfully implements the connection between ASA and TransLAT to minimize the peaking factor for the referenced FA design. The simpler branch of UOX cases have been adjusted so that each one converges to the same final peaking factor solution indicating stability of the method and convergence to a very good optimal solution. This optimal peaking factor solution corresponds to a family of layouts each with their own advantages and disadvantages. Performance characteristics beyond peaking factor results such as reactivity agree with engineering intuition present in literature as well as of the designers of this method. The type of manipulations that are made by the code will typically reduce the reactivity initially given the constraints used in the method. Although this could be viewed as a detractor from using this type of radial enrichment map, it is not necessarily a drawback. Power reactors are often loaded initially with extra reactivity, which is then controlled by adding soluble boron to the moderator material. The lower reactivity produced from these cases indicates that less boron would be necessary to control reactivity. As for the UOX cases that allow Gd-pin insertions, the resulting layouts and outputs also reduce the peaking factor of the FA but do not produce such a large family of solutions. This is to be expected, however, due to the nature of the restrictions necessary to perform the optimization as well as the introduction of the Gd-pins themselves. These restrictions that are put in place limit the

number of pin types that can be inserted in each region, thus reducing the number of permutations of layouts possible. Introducing the Gd-pins and their restrictions further limits the space available for the optimization. These restrictions are, however, not limitations of the code but rather limitations of the physical phenomena and thus lead the optimization process to the optimal domains rather than away from them. Optimal solutions to this sort of analysis are intrinsically bound by the physical phenomena and requirements of the FA itself and thus must be found within the bounds of necessary restrictions on the domain space. For these reasons, the optimal solutions found from the UOX with gadolinium seem feasible solutions given the TransLAT setup and assumptions made. Within the given framework and using the assumptions made, TrASA is a successful implementation of a single objective simulated annealing approach to FA optimization for both branches proposed here.

6.4 FUTURE WORK

TrASA is a continuing work in progress, and it is assumed that it will take many different forms before a useable product can be introduced into the nuclear industry. Several of the shortcomings of the code could be mitigated through further study and research. The most time consuming element of the optimization method, the physics engine that produces the peaking factor, could be replaced by several other heuristic approaches like a properly trained neural network such as those discussed in Souza and Moreira (2006), Jang et al. (2001), Gozalvez (2006), and Ergezinger (1995) or by a streamlined method that calculates only the necessary properties of proposed FA layouts. Integration with these alternatives to using TransLAT as the physics engine is seen as

future work possible for this method. As for the SA side of the methodology, improvements could be made in further adapting ASA to the FA optimization. This might require a keener sense of SA methods and possibly a more streamlined approach to implementing SA.

REFERENCES

Asou, M., Porta, J., 1997. Prospects for poisoning reactor cores of the future. Nuclear Engineering and Design 168, 261-270.

Caprioli, S., 2004. In-core fuel managements for PWRs: Investigation on solutions for optimal utilization of PWR fuel through the use of fuel assemblies with differently enriched ^{235}U fuel pins. Master of Science Thesis, Department of Reactor Physics, Chalmers University of Technology in Sweden, August.

Castillo, A., Gustavo, A., Morales, L.B., Martin-del-Campo, C., Francois, J.L., del Valle, E., 2004. BWR fuel reloads design using a tabu search technique. Annals of Nuclear Energy 31, 151-161.

Ergezinger, S., 1995. An accelerated learning algorithm for multilayer perceptrons: Optimization layer by layer. IEEE Transactions on Neural Networks 6, 1, 31-42.

Gozalvez, J.M., Yilmaz, S., Alim, F., Ivanov, K., Levine, S.H., 2006. Sensitivity study on determining an efficient set of fuel assembly parameters in training data for designing of neural networks in hybrid genetic algorithms. Annals of Nuclear Energy 33, 457-465.

Grossbeck, M.L., Renier, J.P.A., Bigelow, T., 2003. Development of improved burnable poisons for commercial nuclear power reactors. Department of Nuclear Engineering, The University of Tennessee, Final Report on NERI project 99-0074, September.

Haibach, B.V., Feltus, M.A., 1997. A study on the optimization of integral fuel burnable absorbers using deterministic methods. Annals of Nuclear Energy 24, 835-846.

Ingber, L., 2007. Adaptive Simulated Annealing, v26.23. Available by email from ingber@ingber.com or on http://www.ingber.com.

Jang, C.S., Shim, H.J., Kim, C.H., 2001. Optimization layer by layer networks for in-core fuel management optimization computations in PWRs. Annals of Nuclear Energy 28, 1115-1132.

Kirkpatrick, S., Gelatt, C.D., Vecchi, M.P., 1983. Optimization by simulated annealing. Science, 220.4598, 671-680.

Maldonado, G.I., Guo, T., Engrand, P.R., 1998. Dual-objective simulated annealing applied to within-lattice loading optimization. Transactions of the American Nuclear Society 78, 236-237.

Maldonado, G.I., 1998. Penalty-based constraints applied to within-bundle loading optimization. Transactions of the American Nuclear Society 78, 235-236.

Martin-del-Campo, C., Francois, J.L., Carmona, R., Oropeza, I.P., 2007. Optimization of BWR fuel lattice enrichment and gadolinia distribution using genetic algorithms and knowledge. Annals of Nuclear Energy 34, 248-253.

Oconee Nuclear Station 2005. Final Safety Analysis Report, December.

Sanders, C.E., Wagner, J.C., 2002. Study of the effect of integral burnable absorbers for PWR burnup credit. Oak Ridge National Laboratory, Report to the Nuclear Regulatory Commission No. NUREG/CR-6760, ORNL/TM-2000/321.

Souza, R.M.G.P., Moreira, J.M.L., 2006. Neural network correlation for power peak factor estimation. Annals of Nuclear Energy 33, 594-608.

Turinsky, P.J., Parks, G.T., 1999. Advances in nuclear fuel management for light water reactors. Advances in Nuclear Science and Technology 26, 137-165.

Wagner, J.C., Parks, C.V., 2002. Parametric study of the effect of burnable poison rods for PWR burnup credit. Oak Ridge National Laboratory, Report to the Nuclear Regulatory Commission No. NUREG/CR-6761, ORNL/TM-2000/373.

Yilmaz, S., Ivanov, K., Levine, S., 2005. Application of genetic algorithm to optimize burnable poison placement in pressurized water reactors. Genetic and Evolutionary Computation Conference, Washington, DC, June 25-29, 1477-1483.

Yilmaz, S., Ivanov, K., Levine, S., Mahgerefteh, M., 2006. Development of enriched Gd-155 and Gd-157 burnable poison designs for a PWR core. Annals of Nuclear Energy 33, 439-445.

Zavaljevski, N. 1990. A model for fuel shuffling and burnable absorbers optimization in low leakage PWRs. Annals of Nuclear Energy 17, 217-220.

APPENDIX

All TransLAT runs were generated using a simple template input deck. This template is then modified to reflect the proposed ASA layout through Perl scripts and then executed with TransLAT. Several assumptions and calculations went into generating this input deck and thus it will be presented here in its entirety. All results presented are generated from this input deck and are relative to the assumptions contained herein. For interpretation of the input deck, refer to the TransLAT documentation.

TransLAT Advanced Particle Transport Software Using Three-Dimensional Deterministic Methods in Arbitrary Geometry, User's Manual, TransWare Enterprises, Inc., San Jose, CA, (Oct. 2000).

```
TTL TransLAT B&W Mk-B10 Fuel / Enr=4.00 / LBP=0 / Case=mkb10-4-4-4
!
!  Integration Parameters
CON:0
TRP:N MOCS2D
TRP:G OFF
!  Operating State Conditions
SYS PD=31.08 TF=811.0 TC=605.0 TM=577.0 PR=2200.0
!
DOP On
!  Fixed Buckling Option
FUM 1,2
!  Material Data (in number densities)
FUE:FUEL  -93.8    4.00              / Fuel- 4.00 w/o U-235
FUE:FUE1  -93.8    4.00              / Fuel- 4.00 w/o U-235
FUE:FUE2  -93.8    4.00              / Fuel- 4.00 w/o U-235
FUE:FUE3  -93.8    3.75    6.00      / Fuel- 3.75 w/o U-235 6.00 w/o Gd
MAT:CLAD  5.84  24000=0.10 26000=0.21 40000=98.24   TAVE=TC /
MAT:CLA2  6.55  24000=0.10 26000=0.21 40000=98.24   TAVE=TC /
PPM  H3BO3  5000 /
      0.0=700./ Initial Concentration of 700 PPM
MOD 1=0.00 /
!
GEO:1
'PC0',3,0,1,1,1,0 /
 'RPP','MOD',1,1,0.72136/
 'RCC','CLAD',1,1,0.5461/
 'RCC','FUEL',1,1,0.4699/
```

```
'PC1',3,0,1,1,1,2 /
  'RPP','MOD',1,1,0.72136/
  'RCC','CLAD',1,1,0.5461/
  'RCC','FUEL',1,1,0.4699/
'PC2',3,0,1,1,1,1 /
  'RPP','MOD',1,1,0.72136/
  'RCC','CLAD',1,1,0.5461/
  'RCC','FUEL',1,1,0.4699/
'PC10',3,0,1,1,1,0 /
  'RPP','MOD',1,1,0.72136/
  'RCC','CLAD',1,1,0.5461/
  'RCC','FUE1',1,1,0.4699/
'PC11',3,0,1,1,1,2 /
  'RPP','MOD',1,1,0.72136/
  'RCC','CLAD',1,1,0.5461/
  'RCC','FUE1',1,1,0.4699/
'PC12',3,0,1,1,1,1 /
  'RPP','MOD',1,1,0.72136/
  'RCC','CLAD',1,1,0.5461/
  'RCC','FUE1',1,1,0.4699/
'PC20',3,0,1,1,1,0 /
  'RPP','MOD',1,1,0.72136/
  'RCC','CLAD',1,1,0.5461/
  'RCC','FUE2',1,1,0.4699/
'PC21',3,0,1,1,1,2 /
  'RPP','MOD',1,1,0.72136/
  'RCC','CLAD',1,1,0.5461/
  'RCC','FUE2',1,1,0.4699/
'PC22',3,0,1,1,1,1 /
  'RPP','MOD',1,1,0.72136/
  'RCC','CLAD',1,1,0.5461/
  'RCC','FUE2',1,1,0.4699/
'PC30',3,0,1,1,1,0 /
  'RPP','MOD',1,1,0.72136/
  'RCC','CLAD',1,1,0.5461/
  'RCC','FUE3',1,1,0.4699/
'PC31',3,0,1,1,1,2 /
  'RPP','MOD',1,1,0.72136/
  'RCC','CLAD',1,1,0.5461/
  'RCC','FUE3',1,1,0.4699/
'PC32',3,0,1,1,1,1 /
  'RPP','MOD',1,1,0.72136/
  'RCC','CLAD',1,1,0.5461/
  'RCC','FUE3',1,1,0.4699/
'WH',3,0,1,0,0,0 /
  'RPP','MOD',1,1,0.72136/
  'RCC','CLA2',1,1,0.6731/
  'RCC','MOD',1,1,0.65278/
'WH1',3,0,1,0,0,1 /
  'RPP','MOD',1,1,0.72136/
```

```
 'RCC','CLA2',1,1,0.6731/
 'RCC','MOD',1,1,0.65278/
'IT',3,0,1,0,0,4 /
 'RPP','MOD',1,1,0.72136/
 'RCC','CLA2',1,1,0.62611/
 'RCC','MOD',1,1,0.56007/
'WG1',1,0,1,0,0,1 /
 'RPP','MOD',1,1,0.042545/
/
GEO:2
'WG2',1,0,1,0,0,0 /
 'RPP','MOD',1,1,0.72136,0.72136,2*0.042545/
'WG3',1,0,1,0,0,2 /
 'RPP','MOD',1,1,0.72136,0.72136,2*0.042545/
/
LAT
+IT:1
0,0,0,270 /
+PC1:2
1.44272,0,0,270 /
+PC1:3
2.88544,0,0,270 /
+PC1:4
4.32816,0,0,270 /
+PC1:5
5.77088,0,0,270 /
+PC1:6
7.2136,0,0,270 /
+PC1:7
8.65632,0,0,270 /
+PC1:8
10.09904,0,0,270 /
+PC2:9
1.44272,1.44272,0,270 /
+PC0:10
2.88544,1.44272,0,0 /
+PC0:11
4.32816,1.44272,0,0 /
+PC0:12
5.77088,1.44272,0,0 /
+PC0:13
7.2136,1.44272,0,0 /
+PC0:14
8.65632,1.44272,0,0 /
+PC0:15
10.09904,1.44272,0,0 /
+WH1:16
2.88544,2.88544,0,270 /
+PC0:17
4.32816,2.88544,0,0 /
```

```
+PC0:18
5.77088,2.88544,0,0 /
+WH:19
7.2136,2.88544,0,0 /
+PC0:20
8.65632,2.88544,0,0 /
+PC0:21
10.09904,2.88544,0,0 /
+PC2:22
4.32816,4.32816,0,270 /
+PC0:23
5.77088,4.32816,0,0 /
+PC0:24
7.2136,4.32816,0,0 /
+PC0:25
8.65632,4.32816,0,0 /
+PC0:26
10.09904,4.32816,0,0 /
+WH1:27
5.77088,5.77088,0,270 /
+PC0:28
7.2136,5.77088,0,0 /
+PC0:29
8.65632,5.77088,0,0 /
+PC0:30
10.09904,5.77088,0,0 /
+PC2:31
7.2136,7.2136,0,270 /
+PC0:32
8.65632,7.2136,0,0 /
+PC0:33
10.09904,7.2136,0,0 /
+PC2:34
8.65632,8.65632,0,270 /
+PC0:35
10.09904,8.65632,0,0 /
+PC2:36
10.09904,10.09904,0,270 /
+WG1:37
10.862945,10.862945,0,270 /
+WG3:38
10.862945,0,0,270 /
+WG2:39
10.862945,1.44272,0,270 /
+WG2:40
10.862945,2.88544,0,270 /
+WG2:41
10.862945,4.32816,0,270 /
+WG2:42
10.862945,5.77088,0,270 /
```

```
+WG2:43
10.862945,7.2136,0,270 /
+WG2:44
10.862945,8.65632,0,270 /
+WG2:45
10.862945,10.09904,0,270 /
/
! TRA
!  1, 1, 400, 50, 200, 1.5, 'mkb10fa', '/home/translat/tfx/tramcnp_vi.dat'/
!
!   Power Distribution Maps
MAP
'MAPS',1,3,3,0,  0,0,0,0,0,0,0/
8,8,1 /
1,1,'IT:1'/
1,2,'PC1:2'/
1,3,'PC1:3'/
1,4,'PC1:4'/
1,5,'PC1:5'/
1,6,'PC1:6'/
1,7,'PC1:7'/
1,8,'PC1:8'/
2,1,'PC1:2'/
2,2,'PC2:9'/
2,3,'PC0:10'/
2,4,'PC0:11'/
2,5,'PC0:12'/
2,6,'PC0:13'/
2,7,'PC0:14'/
2,8,'PC0:15'/
3,1,'PC1:3'/
3,2,'PC0:10'/
3,3,'WH1:16'/
3,4,'PC0:17'/
3,5,'PC0:18'/
3,6,'WH:19'/
3,7,'PC0:20'/
3,8,'PC0:21'/
4,1,'PC1:4'/
4,2,'PC0:11'/
4,3,'PC0:17'/
4,4,'PC2:22'/
4,5,'PC0:23'/
4,6,'PC0:24'/
4,7,'PC0:25'/
4,8,'PC0:26'/
5,1,'PC1:5'/
5,2,'PC0:12'/
5,3,'PC0:18'/
5,4,'PC0:23'/
```

```
5,5,'WH1:27'/
5,6,'PC0:28'/
5,7,'PC0:29'/
5,8,'PC0:30'/
6,1,'PC1:6'/
6,2,'PC0:13'/
6,3,'WH:19'/
6,4,'PC0:24'/
6,5,'PC0:28'/
6,6,'PC2:31'/
6,7,'PC0:32'/
6,8,'PC0:33'/
7,1,'PC1:7'/
7,2,'PC0:14'/
7,3,'PC0:20'/
7,4,'PC0:25'/
7,5,'PC0:29'/
7,6,'PC0:32'/
7,7,'PC2:34'/
7,8,'PC0:35'/
8,1,'PC1:8'/
8,2,'PC0:15'/
8,3,'PC0:21'/
8,4,'PC0:26'/
8,5,'PC0:30'/
8,6,'PC0:33'/
8,7,'PC0:35'/
8,8,'PC2:36'/
/
!   Print Options
PRI
 1/
 80,1,3,1,0/
/
EDT
 'Assembly','CELL',4,0,1,1,0,0/
/
! Burnup Calculations
!BUR bumax=70 modebu=1 BAMAX=10 BADE1=.25 BADE2=.50/
!
STA
```

VITA

Timothy James Rogers received his Bachelor of Science in Nuclear Engineering from Texas A&M University at College Station in 2006. He then entered the Masters degree program at Texas A&M University at College Station in September 2006 and then went on to receive the Master of Science degree in August 2008. His research interests include, but are not limited to, optimization methods of the stochastic nature including simulated annealing, neural networks, and genetic algorithms. He plans on joining Duke Energy in August of 2008 as an Engineer in Nuclear Engineering at the general office in Charlotte, NC.

Mr. Rogers may be reached through the Nuclear Engineering Department located at Texas A&M University Mail Stop 3133, College Station, Texas 77843-3133. His email address is trogers@ne.tamu.edu .